The role of the mantle during crustal extension: Constraints from geochemistry of volcanic rocks in the Lake Mead area, Nevada and Arizona

DAN L. FEUERBACH* } Center for Volcanic and Tectonic Studies, Department of Geoscience, University of Nevada,
EUGENE I. SMITH } Las Vegas, Las Vegas, Nevada 89154
J. D. WALKER } Isotope Geochemistry Laboratory, Department of Geology, University of Kansas, Lawrence, Kansas 66045
J. A. TANGEMAN* }

ABSTRACT

One of the fundamental questions in areas of large-magnitude extension and magmatism is the role of the mantle in the extension process. The Lake Mead area is ideally suited for developing models that link crustal and mantle processes because it contains both mantle and crustal boundaries and it was the site of large-magnitude crustal extension and magmatism during Miocene time. In the Lake Mead area, the boundary between the amagmatic zone and the northern Colorado River extensional corridor parallels the Lake Mead fault system and is situated just to the north of Lake Mead. This boundary formed between 11 and 6 Ma during, and just following, the peak of extension and corresponds to a contact between two mantle domains. During thinning and replacement of the lithospheric mantle in the northern Colorado River extensional corridor, the lithospheric mantle in the amagmatic zone remained intact. Contrasting behavior to the north and south of this boundary may have produced the mantle domain boundary. The domain to the north of the boundary is characterized by mafic lavas with a lithospheric mantle isotopic and geochemical signature (ε_{Nd} = −3 to −9; $^{87}Sr/^{86}Sr$ = 0.706–0.707). To the south of the boundary in the northern Colorado River extensional corridor, lavas have an ocean island basalt (OIB)–mantle signature and appear to have only a minor lithospheric mantle component in their source (ε_{Nd} = 0 to +4; $^{87}Sr/^{86}Sr$ = 0.703–0.705). Mafic lavas of the northern Colorado River extensional corridor represent the melting of a complex and variable mixture of asthenospheric mantle, lithospheric mantle, and crust. Pliocene alkali basalt magmas of the Fortification Hill field represent the melting of a source composed of a mixture of asthenospheric mantle, high U/Pb (HIMU)–like mantle, and lithospheric mantle. Depth of melting of alkali basalt magmas remained relatively constant from 12 to 6 Ma during, and just after, the peak of extension but probably increased between 6 and 4.3 Ma following extension. Miocene and Pliocene low ε_{Nd} and high $^{87}Sr/^{86}Sr$ magmas and tholeiites at Malpais Flattop were derived from a lithospheric mantle source and were contaminated as they passed through the crust. The shift in isotopic values due to crustal interaction is no more than 4 units in ε_{Nd} and 0.002 in $^{87}Sr/^{86}Sr$ and does not mask the character of the mantle source. The change in source of basalts from lithospheric mantle to asthenospheric mantle with time, the OIB character of the mafic lavas, and the HIMU-like mantle component in the source are compatible with the presence of rising asthenosphere, as an upwelling convective cell, or plume beneath the northern Colorado River extensional corridor during extension. The Lake Mead fault system, a major crustal shear zone, parallels the mantle domain boundary. The Lake Mead fault system may locally represent the crustal manifestation of differential thinning of the lithospheric mantle.

INTRODUCTION

In areas of large-scale extension there are fundamental questions regarding the role of the mantle in the extension process, the identification and age of mantle boundaries, and the relation between mantle and crustal boundaries. We use the Lake Mead area of southern Nevada and northwestern Arizona to address these questions. The Lake Mead area is well suited for this purpose because it contains both mantle and crustal boundaries and it was the site of large-magnitude crustal extension and magmatism during Miocene time.

This paper focuses on Miocene and Pliocene mafic volcanoes (SiO_2 < 55%) between 16.4 and 4.7 Ma in the amagmatic zone and the northern Colorado River extensional corridor. First, we present new geochemical data and infer the source of the mafic magmas. Next, we show that crustal interaction (contamination and commingling) with mafic magmas occurred, but that the isotopic values of the lavas are not shifted enough to mask the character of their mantle source. Last, we use the mafic volcanic rocks that span the boundary between the amagmatic zone and the northern Colorado River extensional corridor as "a probe" into the mantle to determine (1) isotopic differences across the boundary, (2) the age of the boundary, and (3) any link between crustal and mantle processes.

The Lake Mead area contains the boundary between the Western Great Basin and Basin-Range mantle provinces (Menzies and others, 1983; Fitton and others, 1991) and the contact between asthenospheric (OIB) and lithospheric (EM2) mantle domains (Menzies, 1989) (Fig. 1). Mafic volcanic rocks in the Basin-Range mantle province have ε_{Nd} between +5 and +8 and initial $^{87}Sr/^{86}Sr \approx$ 0.703 (Perry and others, 1987; Menzies and others, 1983; Farmer and others, 1989). In contrast, the Western Great Basin province is distinguished by $^{87}Sr/^{86}Sr$ > 0.706 and ε_{Nd} between 0 and −11 (Menzies and others, 1983; Fitton and others, 1988, 1991). Mafic volcanic rocks of the Sierra Nevada mantle province (Fig. 1) (Leeman, 1970; Menzies and others, 1983; Fitton and others, 1988) are isotopically identical to those of the Western

*Present address: Feuerbach: Department of Geology, University of Iowa, Iowa City, Iowa 52242; Tangeman: Department of Geological Sciences, University of Michigan, Ann Arbor, Michigan 48109.

Geological Society of America Bulletin, v. 105, p. 1561–1575, 11 figs., 2 tables, December 1993.

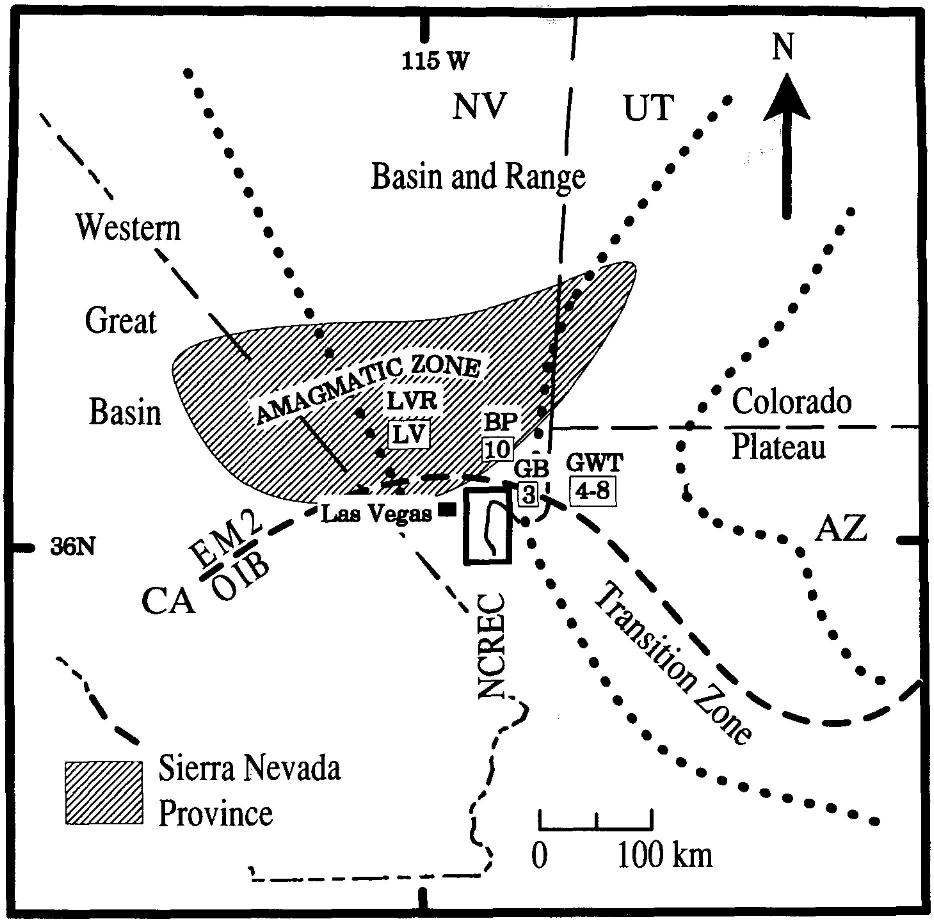

Figure 1. Major mantle and crustal provinces in the southern Basin and Range. The boundaries of the Western Great Basin province are from Fitton and others (1991). Mafic lavas in the Sierran province (Menzies and others, 1983) are identical in isotopic signature to those in the Western Great Basin province. Boundary between EM2 and OIB mantle is from Menzies (1989). Other geologic boundaries are from Fitton and others (1991). The Northern Colorado River extensional corridor (NCREC) was originally defined by Faulds and others (1990). Map also shows the location of sample stations in the Grand Wash trough (GWT), at Gold Butte (GB), Black Point (BP), and in the Las Vegas Range (LVR) (numbers or letters in boxes correspond to first two digits of sample numbers in Table 1). Rectangle indicates area represented in Figure 2.

Great Basin province. Basalts with high $^{87}Sr/^{86}Sr$ and low ε_{Nd} described by Farmer and others (1989) in southern Nevada lie within the Western Great Basin province.

Several important crustal structures pass through the Lake Mead area (Fig. 1). Among these are the Lake Mead fault system (Anderson, 1973; Bohannon, 1979, 1984), a northeast-trending set of left-lateral strike-slip faults, and the Las Vegas Valley shear zone, a northwest-striking set of right-lateral strike-slip faults (Longwell, 1960; Longwell and others, 1965; Duebendorfer and Wallin, 1991). Segments of the Las Vegas Valley shear zone and the Lake Mead fault system define the boundary between the amagmatic zone and the northern Colorado River extensional corridor (Faulds and others, 1990) (Fig. 1). The Lake Mead fault system also separates two regions that have undergone different amounts of extension. To the south of the Lake Mead fault system, in the northern Colorado River extensional corridor, crust was extended by a factor of three to four. To the north, in the amagmatic zone, crust was extended by a factor of two (Wernicke and others, 1988).

The amagmatic zone is a region between 36° and 37° north latitude of minor igneous activity that separates the Great Basin from the Colorado River sections of the Basin and Range province. This zone corresponds to a regional southerly topographic slope and a gravity gradient with an amplitude of about 100 mgals (Eaton, 1982; Eaton and others, 1978). The zone also represents a boundary between contrasting migration directions of magmatism and extension (Glazner and Supplee, 1982; Reynolds and others, 1986; Taylor and Bartley, 1988). In addition to these structures, a major lithospheric boundary defined by Nd mapping of Proterozoic basement rocks trends north-south to the east of the Colorado River (Bennett and DePaolo, 1989). To the west of the boundary in the Lake Mead area, Proterozoic rocks are characterized by model ages of 2.0–2.3 Ga. To the east of the boundary, older basement rocks are 1.8 to 2.0 Ga.

Volcanic rocks in the amagmatic zone are limited to low-volume Pliocene basalt centers at Black Point and in the Las Vegas Range and moderate volume basaltic andesite volcanoes on Callville Mesa (Feuerbach and others, 1991) (Figs. 1 and 2). In the eastern part of the Lake Mead area at Gold Butte, and in the Grand Wash trough, are numerous late Cenozoic alkali basalt centers (Cole, 1989) (Fig. 1). Adjacent to, and within, the Lake Mead fault system is the middle to late Miocene Hamblin-Cleopatra volcano (Thompson, 1985; Barker and Thompson, 1989), the Boulder Wash volcanic section (Naumann, 1987), and flows of late Miocene basalt interbedded with Tertiary sediments near Government Wash north of Lake Mead (Fig. 2). The area south of the Lake Mead fault system contains numerous Miocene and Pliocene volcanic centers (Fig. 2). The most notable of the Miocene centers are in the River Mountains (Smith, 1982), McCullough Range (Smith and others, 1988), Eldorado Mountains (Anderson, 1971), Black Mountains (Faulds and others, 1990), Hoover Dam (Mills, 1985), at Malpais Flattop (Faulds and others, 1991), and in the White Hills (Cascadden, 1991) (Fig. 1). Pliocene centers compose the Fortification Hill volcanic field that extends discontinuously from near Willow Beach, Arizona, to Lake Mead (Fig. 2). In the Lake Mead area, for the most part, volcanism preceded block tilting related to regional extension (9 to 12 Ma; Duebendorfer and Wallin, 1991). Calc-alkaline intermediate lavas were erupted between 18.5 and ~11 Ma. Low-volume basaltic andesite (10.3 to 8.5 Ma), tholeiitic basalt (9.7 to 10.6 Ma), and alkalic basalt (4.3 to 6 Ma) mainly postdate extension (Smith and others, 1990).

ANALYTICAL TECHNIQUES

Whole-rock major-element concentrations were determined by Inductively Coupled

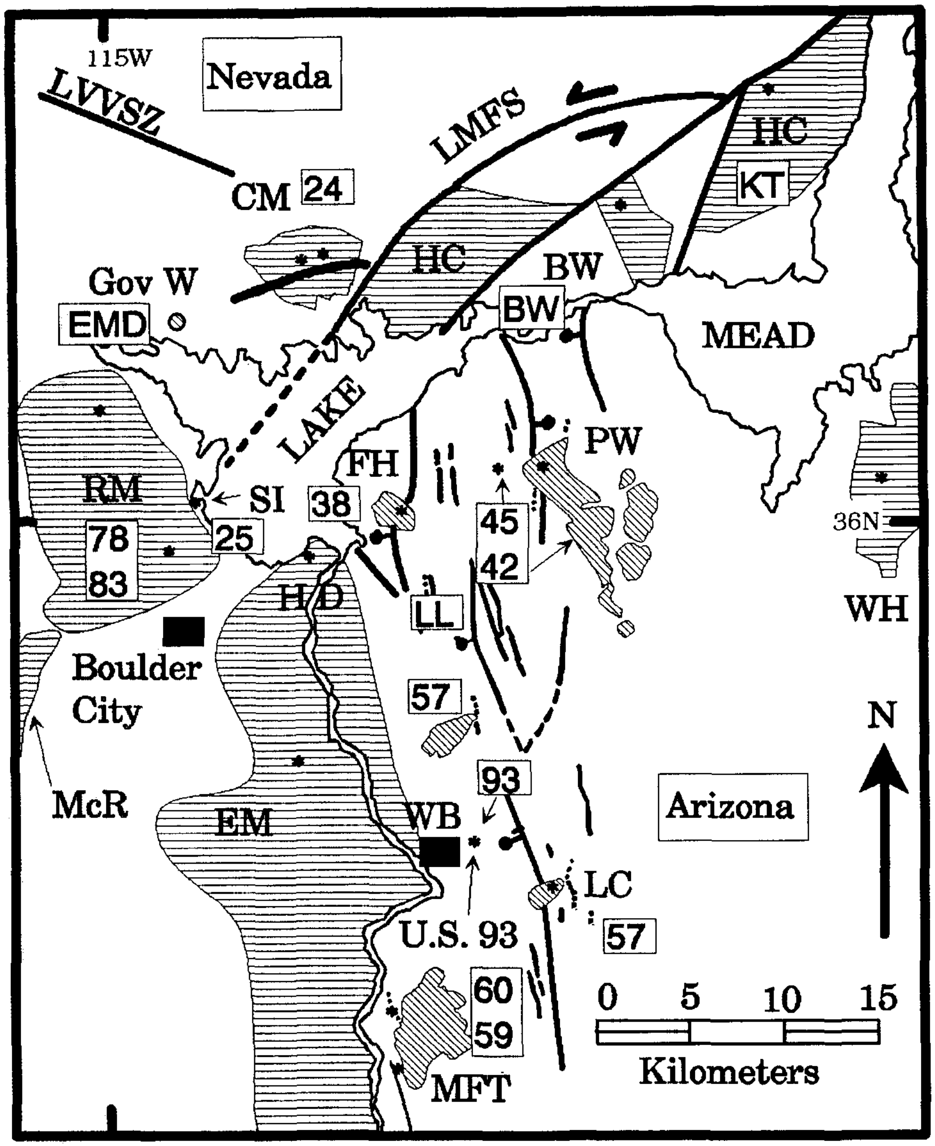

Figure 2. Detailed index map of Lake Mead area and Northern Colorado River extensional corridor showing geologic features mentioned in the text and the location of sample stations (numbers in boxes correspond to first two digits of sample numbers in Table 1). CM, Callville Mesa; BW, Boulder Wash; EM, Eldorado Mountains; HC, Hamblin-Cleopatra volcano; PW, Petroglyph Wash; FH, Fortification Hill; SI, Saddle Island; LC, Lava Cascade; HD, Hoover Dam; WB, Willow Beach; MFT, Malpais Flattop; Gov W, Government Wash; U.S. 93, exposures of alkali basalt along U.S. Route 93; LMFS, Lake Mead fault zone; LVVSZ, Las Vegas Valley shear zone; WH, White Hills; RM, River Mountains; McR, McCullough Range.

Plasma techniques (ICP) at Chemex Labs, Inc. (Sparks, Nevada). Rare-earth elements and Cr, V, Sc, Co, Ta, Hf, and Th were analyzed by Instrumental Neutron Activation Analysis (INAA) at the Phoenix Memorial Laboratory, University of Michigan. The multi-element standards G-2, GSP-1, BHVO-1, and RGM-1 were used as internal standards. Ba, Rb, Ni, and Sr were determined by atomic absorption, and Nb and Sr were analyzed by X-ray fluorescence (XRF) at Chemex Labs, Inc. Rb and Sr were determined by isotope dilution for samples that were analyzed for Nd, Sr, and Pb isotope concentrations. Ni, Nb, Rb, Sr, Zr, Y, and Ba for Fortification Hill basalt were analyzed by XRF at the U.S. Geological Survey's analytical laboratory in Menlo Park, California. This study includes 27 new isotopic analyses from 11 volcanic sections, which represent all major volcanic centers, and a fairly complete sample of mafic volcanic rocks in the Lake Mead area.

Samples for isotopic analysis were dissolved at about 180 °C in a sealed bomb using a HF/HNO_3 mixture. Samples were total-spiked for Rb, Sr, Nd, and Sm. Separation of Rb, Sr, and REE group elements was done using standard cation exchange techniques. The HDEHP-on-Teflon method of White and Patchet (1984) was used for separation of Sm and Nd. The HBr and HNO_3 methods were used for separation of Pb and U, respectively, on aliquots from the whole rock solution. All isotopic analyses were done on a VG Sector 54 mass spectrometer at the University of Kansas. Analyses of Sr and Nd were done in dynamic multicollector mode with ^{88}Sr = 4V and ^{144}Nd = 1V; Rb and Sm were analyzed in static multicollector mode with ^{87}Rb = 200 mV and ^{147}Sm = 500 mV. Analyses for Sr and Sm were done on single Ta filaments; Rb was run on single Re filaments. Nd was run both as NdO^+ and Nd^+. Analytical blanks were less than 100 pg for all elements. Strontium isotopic compositions are normalized for $^{86}Sr/^{88}Sr = 0.1194$ and referenced to NBS-987 $^{87}Sr/^{86}Sr = 0.710250$. Reproducibility of Sr values during these runs was better than ±0.000020 based on replicate runs of NBS-987. Neodymium isotopic compositions are normalized to $^{146}Nd/^{144}Nd = 0.7219$ and referenced to LaJolla $^{143}Nd/^{144}Nd = 0.511850$. Epsilon values for Nd at crystallization are calculated using $(^{143}Nd/^{144}Nd)_{(CHUR,\ 0\ Ma)} = 0.512638$ and $^{147}Sm/^{144}Nd_{(CHUR,\ 0\ Ma)} = 0.1967$. Reproducibility of Nd values are about 0.25 epsilon values based on replicate analyses of LaJolla and inhouse standards. Lead isotopic analyses are referenced to NBS-981 (common Pb) $^{207}Pb/^{206}Pb = 0.91464$ and are corrected for 0.10%/amu fractionation. Fractionation uncertainty is ±0.05%/amu (for example, ±0.08 for $^{208}Pb/^{204}Pb$, ±0.04 for $^{207}Pb/^{204}Pb$, and ±0.04 for $^{206}Pb/^{204}Pb$). Isotope dilution data for Sr, Rb, and Nd are reported in Table 1.

VOLCANOLOGY

Volcanic Rocks of the Northern Colorado River Extensional Corridor

Fortification Hill Field. Fortification Hill basalt crops out in a 50-km-long by 30-km-wide north-northeast elongate area that extends from Lava Cascade, Arizona, to Lake Mead (Fig. 2). We divide the Fortification Hill basalts into older and younger alkalic basalts (OAB and YAB, respectively) based on

TABLE 1. SELECTED ISOTOPIC AND GEOCHEMICAL DATA FROM THE VOLCANIC ROCKS IN THE LAKE MEAD AREA

Sample	U.S. 93	Petroglyph Wash			Maipais Flattop	Fortification Hill	Lava Cascade		Petroglyph Wash	Fortification Hill	Black Point	
	YAB 93-96	YAB 45-124	YAB 42-76	YAB 25-2	TH 60-04	OAB-hy 38-13	OAB 57-113	OAB 57-107	OAB 42-82	OAB 38-143	OAB 10-121	OAB 10-120
SiO_2	44.05	45.50	45.00	44.90	47.28	45.79	44.15	45.35	47.52	47.97	44.58	46.32
Al_2O_3	15.52	16.89	16.79	16.53	14.95	14.50	15.22	16.71	16.61	16.05	14.35	15.30
FeO	10.46	10.04	10.88	11.14	12.38	12.80	13.38	13.81	10.56	11.87	13.82	13.39
CaO	9.07	8.53	8.78	7.68	8.90	8.38	10.69	11.13	9.79	10.16	6.55	7.93
MgO	5.88	5.94	6.21	5.73	6.82	8.78	8.06	5.54	5.35	5.32	8.76	8.92
Na_2O	3.08	4.78	4.94	4.73	2.92	2.86	2.88	3.15	3.57	3.26	4.17	2.97
K_2O	2.80	2.20	3.70	1.04	1.07	0.84	1.10	1.20	2.11	1.40	0.70	0.90
TiO_2	3.02	2.52	2.54	2.40	1.40	1.41	1.76	2.07	1.76	1.46	1.10	1.16
MnO	0.15	0.19	0.18	0.16	0.19	0.16	0.18	0.19	0.16	0.17	0.19	0.19
P_2O_5	0.78	0.77	0.88	0.72	0.24	0.28	0.52	0.53	0.57	0.49	0.30	0.34
LOI	6.48	1.12	0.60	2.93	0.77	1.48	0.52	0.59	1.42	0.49	3.14	4.11
Total	101.40	98.48	100.65	98.06	96.98	97.34	98.46	100.27	99.50	98.64	97.66	101.53
Trace and rare-earth elements in ppm (instrumental neutron activation analysis [INAA], isotope dilution [ID], atomic absorption [AA], X-ray fluorescence spectrometry [XRF])												
Cr(INAA)	103		113	139	242	361	268	80	50	70	271	326
Co(INAA)	25	28	30	29	41	53	43	35	32	33	56	54
Sc(INAA)	15.2	17.4	18.6	18.0	30.0	26.5	30.2	0.0	25.0	26.3	24.5	24.7
V(INAA)		192	216	186	221	213	229	245	281	236	194	177
Hf(INAA)	7.16	6.98	7.22	6.45	3.57	3.38	3.26	4.51	4.00	4.18	1.70	2.83
Th(INAA)	6.08	12.05	12.40	8.51		2.87	3.15	3.66	5.28	3.23		1.16
Ta(INAA)	4.81	5.68	0.00	4.02		1.69	1.66	2.07	1.87	1.31	0.95	
La(INAA)	53.1	85.5	75.1	59.9	14.9	24.6	32.1	37.2	37.7	32.7	12.6	11.8
Ce(INAA)	107.0	140.9	151.0	116.3	35.7	52.4	59.2	69.7	72.3	57.5	24.3	24.7
Sm(INAA)	8.5	8.9	8.6	8.8	3.9	4.8	5.3	6.0	6.2	5.5	3.1	3.1
Eu(INAA)	2.3	2.4	2.3	2.4	1.1	1.6	1.5	1.6	1.6	1.5	0.9	1.1
Yb(INAA)	2.1	2.1	2.4	2.8	2.6	2.2	2.8	2.6	2.5	2.5	1.8	2.3
Lu(INAA)	0.3	0.4	0.2	0.3	0.3		0.3	0.4	0.4	0.4	0.3	0.2
Sr(AA)	1020	820	874	870	274	455	451	464	598	550	246	260
Rb(AA)	34	64	42	22	16	10	10	11	22	14	9	13
Ba(AA)	880	880	0	744	280	475	480	536	800	690	176	190
Ni(AA)	66	70	68	64	84	166	126	42	30	24	206	
Nb(XRF)	68	84	85	63	13	28	30	36	34	28	13	10
Zr(XRF)	285		300	260	105	116	140	160	155	138	77	90
Sr(ID)			873.59	999.69	297.25	434.24	451.23	463.93	597.57	491.11	246.12	306.35
Rb(ID)			43.4	20.24	16.69	14.31	9.68	11.09	22.13	14.86	8.98	14.45
Nd(ID)			49.48	46.29	16.72		24.77	27.26	32.26	25.45		11.09
Selected normative minerals												
Nepheline	6	12	21	7	0	0	6	5	5	3.31	7.34	1.3
Hypersthene	0	0	0	0	6	4	0	0	0	0	0	0
Isotopic analysis by mass spectrometry												
$^{143}Nd/^{144}Nd$			0.512824	0.512801	0.512211	0.512595	0.512711	0.512711	0.512603	0.512592	0.512456	0.512520
ϵ_{Nd}			3.63	3.18	−8.33	−0.84	2.2	1.42	−0.69	−0.9	−3.55	−2.3
$(^{87}Sr/^{86}Sr)i$			0.70347	0.70433	0.70758	0.70565	0.70479	0.70479	0.70555	0.70567	0.70793	0.70753
$^{206}Pb/^{204}Pb$			18.741	18.718	17.742	18.194	18.670	18.591	18.263	18.123	17.947	18.033
$^{207}Pb/^{204}Pb$			15.523	15.564	15.531	15.523	15.570	15.555	15.548	15.541	15.499	15.581
$^{208}Pb/^{204}Pb$			38.476	38.639	38.830	38.309	38.612	38.535	38.397	38.156	38.291	38.9

$Na_2O + K_2O$ (Fig. 3a), light rare-earth-element (REE) enrichment (Fig. 3b), and modal mineralogy. OAB are dated between 5.88 to 4.73 Ma (Feuerbach and others, 1991), and YAB range in age from 4.64 to 4.3 Ma (Anderson and others, 1972; Feuerbach and others, 1991). OAB are mildly alkalic hypersthene (OAB-hy) or nepheline-normative (OAB-ne) olivine-basalts with Ce/Yb mainly between 18 and 46 (Fig. 3b). Nepheline normative alkali basalts from Black Point have Ce/Yb between 7 and about 17 and are surrounded by a dotted line on Figure 3b. OAB lavas erupted from north-northwest–aligned cinder cones on Fortification Hill and from cinder cones at Lava Cascade and in Petroglyph Wash (Fig. 2).

YAB are xenolith-bearing nepheline-normative alkali-olivine basalts with elevated $Na_2O + K_2O$ and Ce/Yb (37 to 68) (Fig. 3b). YAB occurs in three locations: a diatreme at Petroglyph Wash, *en echelon* dikes and a vent along U.S. highway 93, about 10 km south of Hoover Dam, and south of Saddle Island between the North Shore road and Lake Mead (Fig. 2) (Smith, 1984). Ultramafic inclusions and megacrysts of augite and kaersutite are ubiquitous to YAB (Nielson, unpub. data; Campbell and Schenk, 1950). Except for the presence of diorite inclusions in YAB, there is no petrographic evidence of crustal contamination in Fortification Hill lavas.

River Mountains. In the River Mountains (Fig. 2), an andesite-dacite stratovolcano is surrounded by a field of dacite domes (Smith, 1982; Smith and others, 1990). Volcanism occurred in four pulses. The first three are characterized by the eruption of calc-alkaline andesite and dacite flows and the last by rhyolite and alkali basalt. The first episode is associated with the emplacement of a quartz monzonite stock (The River Mountain stock) dated at 13.4 ± 0.5 to 12.8 ± 0.5 Ma (K-Ar biotite dates; Armstrong, 1966, 1970). Anderson and others (1972) reported a K-Ar whole rock date of 12.1 ± 0.5 Ma for a basaltic andesite of the third pulse.

Boulder Wash. Boulder Wash in the northern Black Mountains (Fig. 2) contains a 700-m-thick section of calc-alkaline dacite flows and flow breccias interbedded with flows of pyroxene-olivine andesite containing abundant xenocrysts of quartz and orthoclase (Naumann and Smith, 1987; Naumann, 1987; Smith and others, 1990). Petrographic and textural evidence of magma commingling is well developed in the volcanic section and associated plutonic rocks (Smith and others, 1990; Naumann, 1987). A dacite flow in the eastern part of the volcanic field was dated at 14.2 Ma (K-Ar whole rock date; Thompson, 1985).

Malpais Flattop. Malpais Flattop near Willow Beach, Arizona (Fig. 2) contains a 100-m-thick stack of hypersthene normative tholeiitic basalt flows that erupted from at least two centers now expressed as wide (40 m) dikes and plugs on the west side of the Malpais Flattop mesa (Faulds and others, 1991). Tholeiitic lavas have lower $Na_2O + K_2O$ than alkali basalts with comparable SiO_2 content (Fig. 3a), have lower Ce/Yb than most OAB (Fig. 3b), and are hypersthene normative (Table 1). $^{40}Ar/^{39}Ar$ whole rock

TABLE 1. (*Continued*)

Las Vegas Range LV-104	Callville Mesa		Gold Butte 3-6	Grand Wash Trough		River Mountains				Wilson Ridge LL-88-41	Government Wash EMD-209	Hamblin-Cleopatra Volcano	
	CM 24-68	CM 24-49		4-13	5-14	78-218	78-222	78-223	83-348			KT82-15	KT82-183
42.49	55.18	55.24	46.3	47.58	48.81	47.1	59.0	67.2	72.9	54.1	51.9	56.43	55.89
10.76	15.84	15.98	14.64	14.4	14.95	14.5	16.6	14.2	12.6	16.9	15.2	16.36	16.34
12.79	8.49	8.97	12.59	14.53	11.73	10.9	6.9	3.5	2.7	8.9	9.4	6.76	7.17
9.78	6.64	6.90	7.98	8.74	8.64	11.2	5.5	2.3	0.5	7.4	8.2	6.56	5.4
13.45	4.33	4.10	9.16	8.55	7.14	6.3	2.6	0.9	0.2	4.5	3.8	3.43	3.48
2.39	3.52	3.55	3.16	3	3.22	2.8	3.9	3.6	2.2	4.2	3.7	3.98	4.1
1.00	2.54	2.33	1.59	1.55	1.57	1.8	0.9	0.4	0.2	1.5	1.8	1.31	1.39
1.69	1.07	1.13	1.19	1.25	1.54	1.2	2.3	4.9	7.5	2.1	3.2	2.47	2.72
0.16	0.10	0.14	0.18	0.19	0.16	0.1	0.1	0.1		0.1	0.2	0.1	0.11
0.67	0.30	0.25	0.27	0.26	0.43	1	0.6	0.1		0.7	1.8	0.49	0.49
1.79	2.17	0.40	1.06	0.19	1.09	2.3	1	3	0.1	0.5	1.2	1.38	2.85
96.97	100.25	99.17	98.12	100.24	99.28	99.2	99.4	100.2	98.9	100.9	100.4	99.27	99.94
Trace and rare-earth elements in ppm (instrumental neutron activation analysis [INAA], isotope dilution [ID], atomic absorption [AA], X-ray fluorescence spectrometry [XRF])													
816	134	145	253	326	256						63	47	
58	28	29	46.68	50.49	39.52					20		20.65	22.76
22.2	18.2	19.6	23.73	27	23.91	29.6	11.2	3.8	1.5			14.06	14.11
234	153	171	216	242	215					198		147	145
5.22	4.29	3.86	3.63	3.14	3.24	8.1	7.3	4.8	4.9	5.1		6.76	8.15
5.20	5.46	4.89	2.72		2.78	13.2	14.9	17.6	31.2	12.4		10.46	13.53
0.71	0.96	0.97				1.5	1	1.2	15.3	2.1		2.75	2.84
46.0	34.2	34.0	23.86	9.04	19.21	107.6	81.7	52.4	55.6	123		65.23	
92.0	72.1	67.6	46.11	21.87	44.26	242.4	167.9	90.7	124.5	213		114.03	126.79
10.2	5.2	5.3				15.5	8.7	4.2	3.7	10.9		7.75	8.29
2.3	1.4	1.4	1.45	0.95	1.33	3.9	2	1.2	1	2.6		1.89	1.99
1.7	2.6	2.2	2.47	1.96	2.28	2.1	2.3	1.3	2.2	2.3		1.73	2.04
0.1	0.3	0.3	0.35	0.3	0.24	0.4	0.4	0.2	0.3	0.3			0.26
	424	970											
	51	40											
	880	840											
	60	36											
	17	23											
	145	185											
795.58	423.51	970.19	421.14	321.83	378.36		959.65	467.99	79.76	1155.78	1299.65	432.85	588.44
48.27	50.94	40.1	14.88	7.47	8.06		83.62	129.26	198.08	42.05	75.97	45.83	47.52
55.76	25.97	29.96	22.47	14.35	17.89	98.57	54.9	28.2	22.84	76.018	74.18	45.08	45.27
Selected normative minerals													
5	0	0	5.22	4.34	1.27	3.72	0	0	0	0	0	0	0
0	14	14	0	0	0	0	15.33	2.24	5.87	18.11	17.98	11.07	16.93
Isotopic analysis by mass spectrometry													
0.512269	0.512090	0.512203	0.512592	0.512295	0.512716	0.512210	0.512060	0.512055	0.512008	0.512133	0.512128	0.512390	0.512456
−7.2	−10.69	−8.49	−0.9	−0.27	1.87	−8.34	−11.28	−11.37	−12.28	−9.86	−9.94	−4.84	−3.51
0.70632	0.70792	0.70893	0.70502	0.7046	0.7044	0.708954	0.7082	0.709233	0.710015	0.70815	0.707337	0.70442	0.70562
18.963	17.173	17.332	18.130	17.821	18.127	18.299	17.922	17.885	18.156	17.887	18.16	17.971	18.096
15.642	15.453	15.496	15.527	15.550	15.509	15.605	15.537	15.553	15.578	15.537	15.56	15.515	15.538
38.845	37.814	38.01	38.068	38.050	37.895	38.699	38.791	38.982	38.906	38.725	38.939	38.344	38.549

dates of 9.7 ± 0.5 and 10.6 ± 0.5 Ma were obtained for flows near the top and at the base of the flow stack, respectively (Faulds and Gans, unpub. data).

Eldorado Mountains. A sequence of mafic to felsic volcanic rocks erupted between 18.5 and ~12 Ma in the Eldorado Mountains (Anderson, 1971; Darvall and others, 1991) (Fig. 2). The sequence is divided into a lower section of basaltic andesite (predominant) and rhyolite lavas (Patsy Mine volcanics; Anderson, 1971), and an upper section of basaltic andesite, dacite, and rhyolite (Mount Davis volcanics; Anderson, 1971). Mafic lavas lack petrographic and field textures characteristic of crustal contamination or magma commingling. A similar section of mafic lavas in the White Hills, Arizona (Fig. 1), formed by partial melting of mantle peridotite without significant crustal interaction (Cascadden and Smith, 1991; Cascadden, 1991). In the Eldorado Range, lavas and associated plutonic rocks span the period of most rapid extension. Patsy Mine and the lower parts of the Mount Davis section are tilted nearly 90°. Younger units are rotated less in the same structural blocks (Anderson, 1971).

Hamblin-Cleopatra Volcano. The Hamblin-Cleopatra volcano (14.2–11.5 Ma) (Anderson, 1973; Thompson, 1985), which lies along the north shore of Lake Mead (Fig. 2), is a 60-km^3 stratovolcano composed of shoshonite, latite, trachydacite, and trachyte lava (Barker and Thompson, 1989). In addition, tephra, epiclastic sediments, intrusions, and a well-developed radial dike system form the volcano. The volcano was dismembered into three segments by left-lateral strike-slip faulting associated with the Lake Mead fault system (Anderson, 1973; Thompson, 1985; Barker and Thompson, 1989).

Volcanic Rocks at Gold Butte and in the Grand Wash Trough

The Grand Wash trough and the Gold Butte area (Fig. 2) contain flows, dikes, and plugs of olivine-phyric alkali basalt that locally contain mantle xenoliths (Cole, 1989). Basalt in the Grand Wash trough is dated at 3.99 to 6.9 Ma (K-Ar plagioclase) and is younger than alkali basalt to the west in the Gold Butte area (K-Ar plagioclase dates of 9.15 to 9.46 Ma; Cole, 1989) (Fig. 2).

Volcanic Rocks in the Amagmatic Zone

Callville Mesa. Olivine-clinopyroxene basaltic andesite erupted from compound cinder cones on Callville Mesa and in West End Wash between 10.46 and 8.49 Ma (Feuerbach and others, 1991) (Fig. 2). Basaltic andesite has similar $Na_2O + K_2O$ and Ce/Yb to OAB but has higher SiO_2 (46.83–57.32 wt%) (Fig. 3). Basaltic andesite contains abundant quartz and alkali-feldspar xenocrysts that are rimmed by glass and acicular clinopyroxene (diopsidic-augite).

Black Point. At Black Point on the west shore of the Overton Arm of Lake Mead (Fig. 1), thin flows of nepheline-normative alkali basalts (OAB-ne) (6.02 Ma; Feuerbach and others, 1991) associated with north-striking *en echelon* dikes overlie gypsiferous sediments of the Tertiary Horse Spring

TABLE 1. (*Continued*)

Explanation

YAB—Young alkali basalts of the Fortification Hill field (6–4.3 Ma).
OAB—Older normative nepheline alkali basalts of the Fortification Hill field (6 Ma).
OAB-hy—Older normative hypersthene alkali basalts of the Fortification Hill field (6 Ma).
TH—Tholeiitic basalts from Malpais Flattop, Arizona (10.6–9.7 Ma).

Locality descriptions

Locality	Location (lat., long.)	Age* (Ma)	Description
YAB			
U.S. 93	36°00'00"N 114°45'00"W	4.64–4.3	Volcanic center with numerous dikes. Amphibole megacrysts numerous; mantle xenoliths rare.
Petroglyph Wash	36°04'37"N 114°35'44"W	4.3	Alkali basalt forms a small cylindrical vent. Amphibole megacrysts are common.
Saddle Island	36°02'30"N 114°48'00"W	Not dated	Flow interbedded with Tertiary gravel. Mantle xenoliths are rare.
TH			
Malpais Flattop	35°45'00"N 114°40'00"W	10.6–9.7 ($^{40}Ar/^{39}Ar$ dates)	100-m-thick stack of hypersthene-normative tholeiitic basalt flows with wide dikes.
OAB			
Fortification Hill	36°03'45"N 114°40'56"W	5.89–5.42	Over 80 flows associated with cinder cones and shallow intrusions.
Lava Cascade	35°52'38"N 114°35'15"W	5.16–4.74	Flows and vent zone at summit of Black Mountains.
Petroglyph Wash	36°04'37"N 114°35'44"W	5.43–4.61	Stack of flows related to at least two vents.
Black Point	36°24'43"N 114°23'02"W	6.01	Flows and dikes. Flows interbedded with gypsiferous Tertiary sediments.
Las Vegas Range	36°30'19"N 115°02'30"W	16.4	One or two alkali basalt flows tilted about 20° east extensively covered by Quaternary sediments.
Callville Mesa	36°10'19"N 114°42'30"W	10.46 and 8.49	Olivine-clinopyroxene bearing basaltic-andesite flows erupted from compound cinder cones.
Gold Butte	36°15'00"N 114°15'00"W	9.15–9.46	Flows of alkali basalt along the Gold Butte fault.
Grand Wash trough	36°15'00"N 113°50'00"W	3.99–6.9	Flows, dikes, and plugs of olivine-phyric alkali basalt that locally contain mantle xenoliths.
River Mountains	36°05'00"N 114°50'00"W	13.4–12.1	Andesite-dacite stratovolcano surrounded by a field of dacite domes and a basalt shield.
Wilson Ridge	36°06'21"N 114°37'30"W	13.4	Basalt dikes cutting Wilson Ridge pluton.
Government Wash	36°07'00"N 114°45'00"W	12	80-m-thick section of flows and agglomerates are interbedded with the Lovell Wash member of the Tertiary Horse Spring Formation.
Hamblin-Cleopatra	36°10'00"N 114°36'00"W	14.2–11.5	60 km^3 stratovolcano composed of shoshonite, latite, trachydacite, and trachyte lava. Volcano is cut by a radial dike system.
Boulder Wash	36°07'00"N 114°37'00"W	14.2	700-m-thick section of calc-alkaline dacite flows and flow breccias interbedded with flows of pyroxene-olivine andesite.
Eldorado Mountains (isotope data from Daley and DePaolo, 1992)	35°45'00"N 114°42'00"W	18.5–12 ($^{40}Ar/^{39}Ar$ dates)	A lower section of basaltic-andesite (predominant) and rhyolite lavas and an upper section of basaltic andesite, dacite, and rhyolite. The sections are separated by a dacite ash-flow tuff (tuff of Bridge Spring).

*All dates are K-Ar except where noted.

Formation. Total outcrop area is about 12 km^2.

Las Vegas Range. The Las Vegas Range locality is composed of thin flows of alkali basalt in a fault-bounded basin just to the west of U.S. highway 93 (Fig. 1). Flows (2 km^2) are mostly covered by Quaternary fanglomerate and alluvium, and as a result, no source area was discovered. Basalt in the Las Vegas Range is dated at 16.4 ± 0.6 Ma (K-Ar whole rock date; Smith, unpub. data).

Basalt of Government Wash. Olivine-phyric basalt crops out near Government Wash just north of Lake Mead. A 60- to 80-m-thick section of flows and agglomerates is interbedded with the Lovell Wash member of the Tertiary Horse Spring Formation (Duebendorfer, 1991, personal commun.). Basalt of Government Wash is dated at 12.0 Ma (K-Ar plagioclase date) (Duebendorfer and others, 1991).

SOURCE OF MAFIC LAVAS

Introduction

Crustal contamination is less of a factor for alkalic than tholeiitic rocks, because the former are lower in volume and less likely to reside in upper crustal chambers where open system processes occur. Also, high Sr and light rare-earth-element concentrations of alkalic magmas tend to overwhelm any effects of crustal contamination. Furthermore, alkalic magmas commonly contain mantle xenoliths and apparently rise quickly through the crust with little or no contamination (for example, Glazner and Farmer, 1992). Smith and others (1990) indicated that crustal contamination was an important factor in the production of intermediate lavas of the River Mountains. In this paper, we demonstrate that crustal contamination also affected the mafic lavas at Callville Mesa, hypersthene-normative alkali basalts (OAB-hy) of the Fortification Hill field, and tholeiitic basalts at Malpais Flattop. Although these magmas were con-

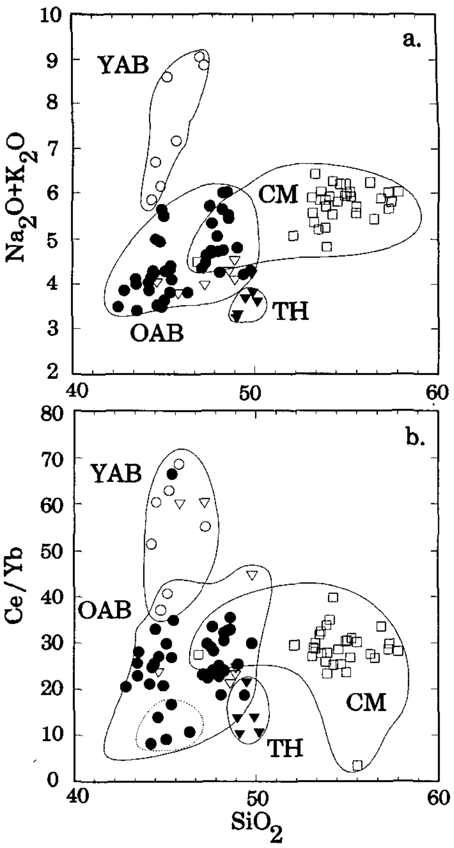

Figure 3. a. Plot of total alkalis (Na_2O + K_2O) versus SiO_2 for volcanic rocks of the Fortification Hill volcanic field, Callville Mesa, Black Point, and Malpais Flattop. Open circles, young alkali basalts (YAB) of the Fortification Hill field; filled circles, older alkali basalts (OAB) of the Fortification Hill field; open triangles, hypersthene normative alkali basalts (OAB-hy) of the Fortification Hill field; filled triangles, tholeiitic basalts (TH) from Malpais Flattop; open boxes, mafic lavas of Callville Mesa (CM).

b. Plot of Ce/Yb versus SiO_2 for volcanic rocks of the Fortification Hill volcanic field, Callville Mesa, Black Point, and Malpais Flattop. Symbols are the same as in Figure 3a. Solid circles surrounded by dotted line are mafic lavas at Black Point.

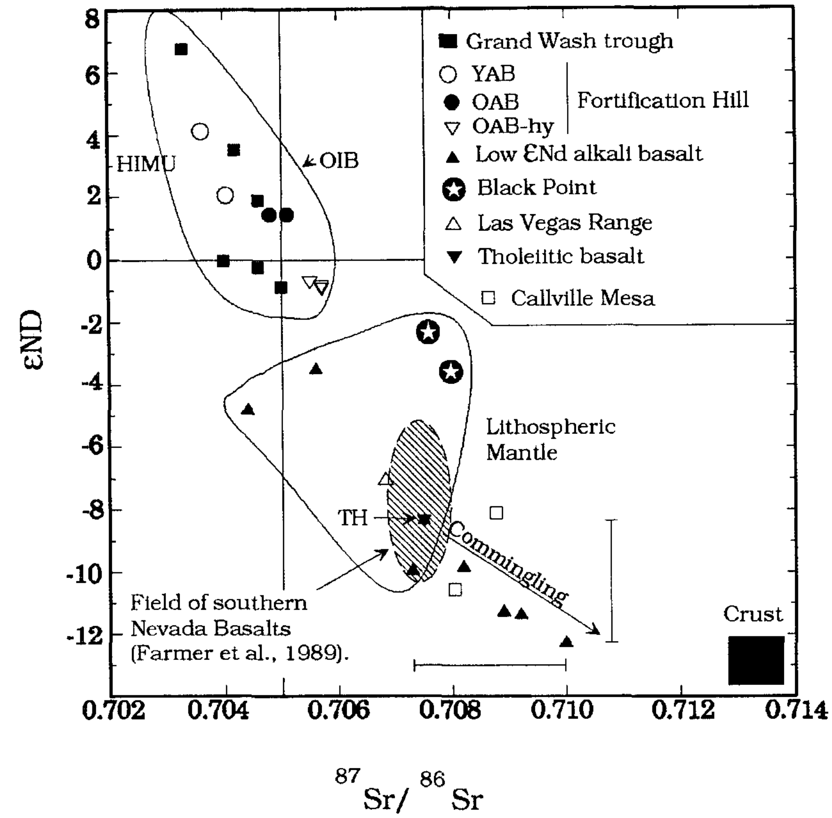

Figure 4. Post–9 Ma alkali basalts in the northern Colorado River extensional corridor are similar to ocean island basalts (OIB) in terms of ε_{Nd} and $^{87}Sr/^{86}Sr$. Pre–9 Ma mafic lavas region wide and post–9 Ma basalts in the amagmatic zone originated in the lithospheric mantle. Lithospheric mantle in the Lake Mead area has a wider range of isotopic compositions than lithospheric mantle reported by Farmer and others (1989) for southern Nevada basalts. In the River Mountains, magma commingling resulted in a change of ε_{Nd} of about 4 units and $^{87}Sr/^{86}Sr$ of about 0.002 (indicated by brackets). DM, depleted mantle (MORB); HIMU, a mantle component with high μ ($^{238}U/^{204}Pb$); OIB, ocean island basalt, TH, tholeiitic basalt.

taminated by crust, we will show that the isotopic shift due to crustal interaction is small when compared to the overall isotopic variation. Therefore, the isotopic composition of these contaminated mafic magmas is not shifted enough by crustal interaction to mask the character of their mantle source. They are still useful for the mapping of mantle domains.

Mantle Source and Crustal Contamination

OAB, YAB, and Grand Wash Trough. YAB and OAB of the Fortification Hill field and alkali basalts of Grand Wash trough have $^{87}Sr/^{86}Sr$ = 0.703–0.706, ε_{Nd} = −1 to +6.7, $^{206}Pb/^{204}Pb$ = 17.8–18.7 and $^{208}Pb/^{204}Pb$ = 38–38.5 (Table 1). These alkali basalts have Nd and Sr isotopic compositions and trace-element distributions that are similar to those of modern-day ocean island basalts (OIB) (Zindler and Hart, 1986; Fitton and others, 1991) (Fig. 4). We suggest that YAB originated from a source dominated by asthenospheric mantle, and as discussed below, OAB melted a mixed asthenospheric mantle–lithospheric mantle source dominated by asthenospheric mantle (Table 2).

When compared to typical OIB and the alkali basalts of the Grand Wash trough, OAB and YAB appear to contain an additional component. YAB and OAB plot between lithospheric mantle and higher values of ε_{Nd} and $^{206}Pb/^{204}Pb$ (Fig. 5) rather than lower Pb and higher ε_{Nd} as do Grand Wash trough basalts. We suggest that the trend toward higher rather than lower Pb is due to the presence of HIMU-like mantle (ε_{Nd} = 3.5, $^{206}Pb/^{204}Pb$ > 20) in the source of OAB and YAB. HIMU-like mantle may reside in either the lithospheric mantle or upper asthenosphere (Zindler and Hart, 1986; Hart, 1988; Hart and others, 1992) or as detached oceanic slabs deep within the mantle (Weaver, 1991b). Weaver (1991b) and Hart and others (1992) suggest that the source of HIMU mantle is in the asthenosphere and that it is incorporated into the OIB source by rising plumes or mantle diapirs. We infer that the presence of this component in OAB and in xenolith-bearing YAB and its higher abundance in xenolith-bearing alkali basalts are more compatible with its residence in asthenospheric mantle than in lithospheric mantle.

OAB-containing normative hypersthene (OAB-hy) are the oldest mafic lavas of the Fortification Hill field and have higher $^{87}Sr/^{86}Sr$ (0.7055–0.7057) and lower ε_{Nd} (−0.68 to −0.9) than the nepheline normative basalts of this group (Fig. 4). Both crustal contamination and the presence of a lithospheric mantle component in the source must be considered as explanations for the lower ε_{Nd} and higher $^{87}Sr/^{86}Sr$ of the OAB-hy lavas. Glazner and Farmer (1992) demonstrated that xenolith-bearing alkali basalts from the Mojave Desert, California, have Sr and Nd isotopic compositions similar to typical OIB, and xenolith-free basalts have a range of compositions that trend from OIB toward values more typical of continental lithosphere. They suggest that these isotopic compositions can be explained if xenolith-bearing magmas passed through the crust quickly without interaction and xenolith-free magmas stopped in the crust long enough for xenoliths to drop or be digested and for crustal interaction to occur. In detail, alkali basalts in the Mojave Desert display a trend toward higher $^{87}Sr/^{86}Sr$ and lower ε_{Nd} with time (Glazner and Farmer,

TABLE 2. SOURCE OF MAFIC VOLCANIC ROCKS IN THE LAKE MEAD AREA

Magma type	YAB	OAB-ne	OAB-hy	TH	Low ε_{Nd} alkali basalts
Components in source	AM + HIMU + LM	AM + HIMU + LM	AM + LM + HIMU	LM + CRUST (contamination)	LM + CRUST (commingling)

Notes: Size of text indicates relative contribution of each component. YAB, young alkali basalts of the Fortification Hill field; OAB-ne and OAB-hy, nepheline- and hypersthene-bearing alkali basalts of the Fortification Hill field; TH, tholeiitic basalts at Malpais Flattop; AM, asthenospheric mantle; LM, lithospheric mantle; HIMU, high uranium ($^{238}U/^{204}Pb$) mantle component.

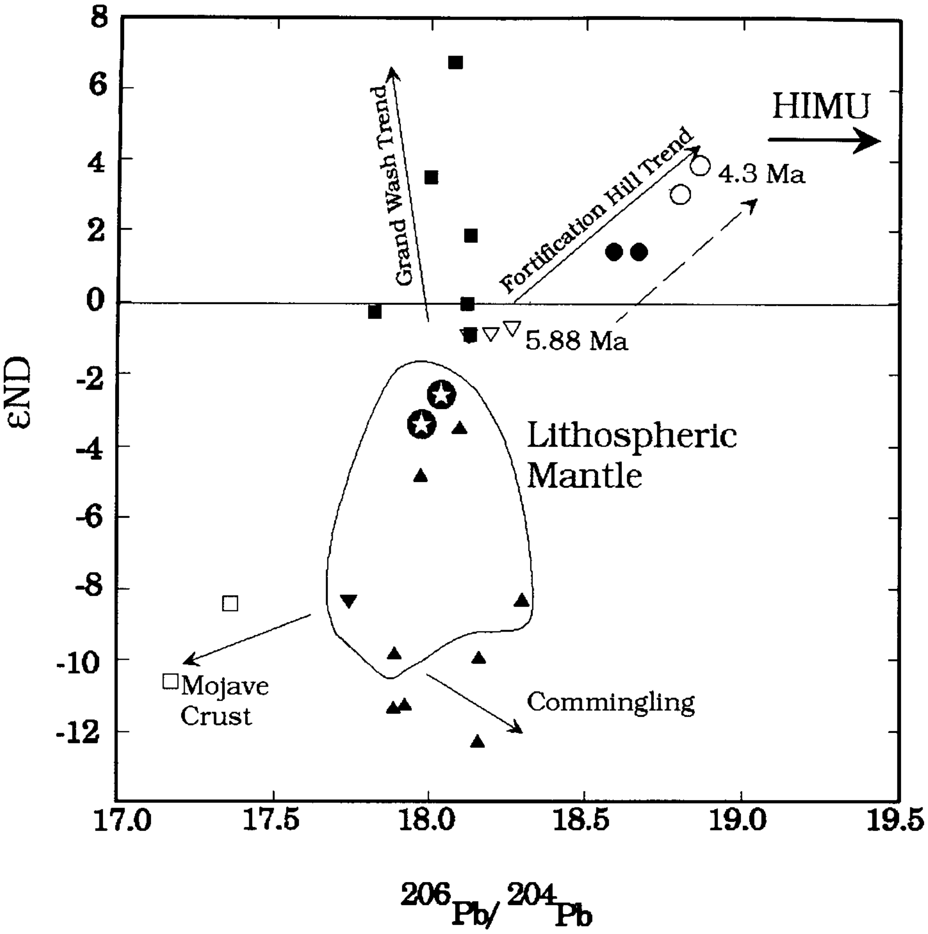

Figure 5. Mafic lavas of the Fortification Hill field appear to contain an HIMU-like component in their source. Fortification Hill basalts define a trend that extends from lithospheric mantle toward HIMU-like mantle. Mafic lavas of the Grand Wash trough lack this component and trend toward typical asthenospheric mantle. Callville Mesa lavas are low in Pb and show the effect of contamination by Mojave-type crust (lower to middle crust). Mafic volcanic rocks in the River Mountains commingled with felsic upper crust and trend toward higher $^{206}Pb/^{204}Pb$. Symbols are defined in Figure 4.

1992). They attributed this trend to the hybridization of asthenospherically derived partial melts by commingling with partial melts of Late Jurassic gabbro and Proterozoic diabase. By this mechanism, ε_{Nd} can be changed by as much as three units without appreciably changing major- or trace-element chemistry. Although it is possible that such a mechanism is active in this area, two observations suggest that the Glazner and Farmer (1992) model does *not* explain the isotopic composition of OAB-hy. First, in the northern Colorado River extensional corridor, a probable mafic crustal contaminant is Proterozoic (1.7 Ga) amphibolite that crops out in the footwall of the Saddle Island detachment (Duebendorfer and others, 1990). Isotopically, the amphibolite has low $^{87}Sr/^{86}Sr_{T = 6\ Ma}$ (0.7029) and high $\varepsilon_{NdT = 6\ Ma}$ (3.18). Therefore, contamination of asthenospherically derived magmas by this type of crust *will probably not* produce OAB-hy or other xenolith-free mafic lavas. Second, OAB-hy are temporally separated from other magma types in the northern Colorado River extensional corridor. This temporal distribution is circumstantial evidence that OAB-hy magmas may sample a different mixture of mantle than OAB-ne or YAB. Therefore, we suggest that OAB-hy and some OAB-ne probably represent a mixture of asthenospheric mantle and lithospheric mantle (Fig. 5) and not cryptic contamination of mafic magmas by crust.

The trend toward higher ε_{Nd}, lower $^{87}Sr/^{86}Sr$, and higher $^{206}Pb/^{204}Pb$ between 6 and 4 Ma (Figs. 4 and 5) suggests that if the source for OAB is a mixture of asthenospheric mantle and lithospheric mantle, then the ratio of lithospheric mantle to asthenospheric mantle is decreasing in the source with time. This relation implies that the source of OAB was near the boundary between asthenospheric mantle and lithospheric mantle and *either* this boundary rose through the source area due to extension-related lithospheric thinning, or the depth of melting increased between 6 and 4.3 Ma. As little upper-crustal extension occurred between 6 and 4.3 Ma (Feuerbach and others, 1991), we prefer the latter model. Alkali basalts are generated from mantle peridotite at pressures between 15 and 20 kbar corresponding to a depth of about 45 to 60 km (Takahashi and Kushiro, 1983). The boundary between lithospheric mantle and asthenospheric mantle beneath the northern Colorado River extensional corridor was probably in this depth range during the Pliocene. Our depth estimate is consistent with the depth of the lithospheric mantle–depleted mantle (asthenosphere) boundary estimated by Daley and DePaolo (1992; Fig. 1) for the same time interval and geographic area.

Low ε_{Nd} Basalts. Low ε_{Nd} alkali basalts occur as pre–11 Ma lavas in the River Mountains, Eldorado Range, Boulder Wash area, Hamblin-Cleopatra volcano, and in the Las Vegas Range, and as post–11 Ma lavas at Callville Mesa and Black Point ($^{87}Sr/^{86}Sr$ = 0.705–0.710 and ε_{Nd} = −4 to −12) (Fig. 4).

Andesite and dacite in the River Mountains show abundant field and petrographic evidence of assimilation and magma commingling (Smith and others, 1990). Alkali basalt lacks evidence of contamination and was considered by Smith and others (1990) to have been generated by partial melting of mantle peridotite. Intermediate lavas in the River Mountains may represent hybrid compositions formed by the commingling of mafic and felsic end members. This interpretation is supported by a positive correlation between $^{87}Sr/^{86}Sr$ and SiO_2 and a negative correlation between ε_{Nd} and SiO_2 (Fig. 6). The isotopic compositions of basalt and rhyolite end members of the mixing sequence provide a quantitative estimate of the magnitude of isotopic shift due to magma commingling (Fig. 4). This shift is no more than four units in ε_{Nd} and 0.002 in $^{87}Sr/^{86}Sr$.

Callville Mesa lavas have $^{87}Sr/^{86}Sr$ = 0.708–0.709 and ε_{Nd} = −8 to −10 and are similar in isotopic composition and trace-element chemistry (high Ba, K, and Sr and low Nb and Ti) to mafic lavas derived from lithospheric mantle in the western United States (Fitton and others, 1991; Farmer and others, 1989). Callville Mesa lavas differ, however,

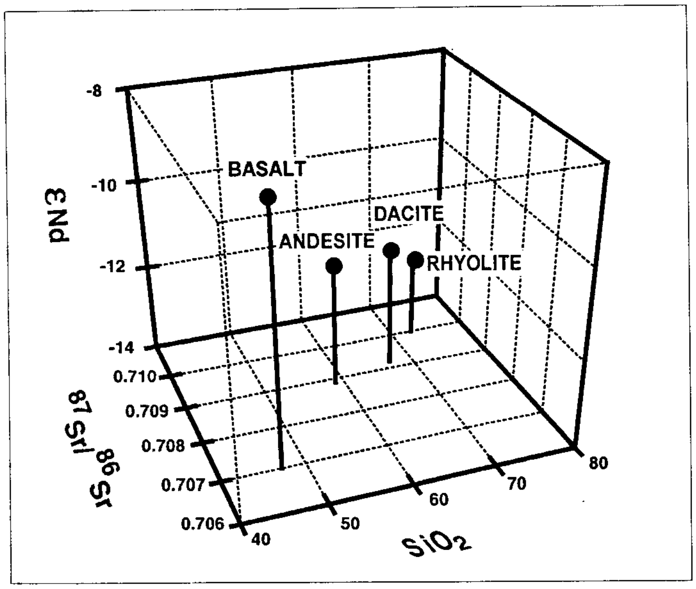

Figure 6. Three-dimensional plot of ε_{Nd} versus $^{87}Sr/^{86}Sr$ versus SiO_2 for volcanic rocks of the River Mountains. The positive correlation between SiO_2 and $^{87}Sr/^{86}Sr$ and the negative correlation between SiO_2 and ε_{Nd} suggest that rhyolite and basalt are end members of a mixing sequence. Intermediate compositions represent the mixing of the end-member compositions in various proportions.

by having lower Pb ratios ($^{207}Pb/^{204}Pb$ = 15.45–15.5; $^{208}Pb/^{204}Pb$ = 37.7–38; $^{206}Pb/^{204}Pb$ = 17.2–17.4) than typical lithospheric-mantle–derived basalts ($^{207}Pb/^{204}Pb$ = 15.6; $^{208}Pb/^{204}Pb$ = 38.7; $^{206}Pb/^{204}Pb$ = 18.3) (Fig. 5); having trends on Rb/Sr, Th/Nb, and La/Nb versus SiO_2 plots that project toward crustal compositions (Figs. 7a, 7b, and 7c); and by displaying ample evidence of crustal contamination. These geochemical and petrographic features suggest that Callville magmas were contaminated by the crustal material. The crustal component has $^{87}Sr/^{86}Sr > 0.710$, low Pb isotope ratios, and $\varepsilon_{Nd} < -10$ (Fig. 5). We suggest that the crustal contaminant is similar in chemistry to Proterozoic rocks of the Mojave crustal province, which extends into the Lake Mead area (Wooden and Miller, 1990). Although rocks of the Mojave province display a wide range of Pb isotope values, low ratios ($^{207}Pb/^{204}Pb < 15.5$; $^{208}Pb/^{204}Pb < 38$; $^{206}Pb/^{204}Pb < 17.4$) are common. Because of the common occurrence of quartz and alkali feldspar xenocrysts in Callville Mesa lavas, the contaminant is inferred to be a felsic rock. Uncontaminated magma at Callville Mesa is similar in major- and trace-element composition to OAB. A normative nepheline-bearing alkali basalt (sample 24-100; Table 1), the oldest flow recognized from the Callville Mesa center, plots in the field of OAB in terms of $Na_2O + K_2O$ (Fig. 3a), Ce/Yb (Fig. 3b), and trace-element ratios (Fig. 7).

Tholeiitic Basalt. Tholeiitic basalts at Malpais Flattop have high Sr ($^{87}Sr/^{86}Sr = 0.7075$), low ε_{Nd} (−8.33), and increasing Rb/Nb, Th/Nb, and La/Nb (Figs. 7a, 7b, and 7c). These lavas may have been contaminated as they passed through the crust. It is generally accepted that tholeiitic basalts equilibrate at shallower depths in the mantle than alkali basalts (24 to 45 km; Takahashi and Kushiro, 1983). If OAB were generated near the lithospheric mantle–asthenospheric mantle boundary as suggested above, it is reasonable to conclude that the tholeiitic basalts were produced by melting of lithospheric mantle. Tholeiitic basalts in the western United States are generally assumed to have been affected by small amounts of crustal contamination as well as fractional crystallization (Dungan, 1992). The close spatial and temporal association of alkali and tholeiitic basalts, lack of mantle xenoliths, together with isotopic and chemical signatures support the contamination hypothesis (for example, Perry and others, 1987; Glazner and Farmer, 1992). To estimate the changes in isotopic composition of lithospherically derived magmas due to crustal contamination, we compared tholeiitic basalts to alkali basalt derived in the lithospheric mantle (for example, Las Vegas Range alkali basalt to Malpais Flattop tholeiite). Tholeiitic basalts have higher $^{87}Sr/^{86}Sr$ and lower ε_{Nd} than alkali basalts ($^{87}Sr/^{86}Sr$ = 0.0007 higher; ε_{Nd} = 1.13 lower). Other investigators noted similar isotopic changes due to crustal contamination. For example, Glazner and Farmer (1992) noted a shift in ε_{Nd} by as much as three units as the result of contamination of mafic magmas by mafic crust. Daley and DePaolo (1992) estimated that ε_{Nd} may be lowered by 2 to 3 units by crustal contamination. Crowley (1984) demonstrated a shift in $^{87}Sr/^{86}Sr$ by as much as 0.001 when comparing tholeiites and alkali basalts derived from the lithospheric mantle. On the basis of our data and the work of others, we conclude that the isotopic compositions of tholeiitic basalt reflect the melting of enriched mantle (lithospheric mantle) and that the changes in ε_{Nd} (1 to 3 units) and $^{87}Sr/^{86}Sr$ (0.001) due to crustal contamination are small when compared to overall variations of ε_{Nd} and $^{87}Sr/^{86}Sr$ between these rocks and the alkali basalts.

Summary

Mafic lavas of the northern Colorado River extensional corridor represent the melting of a complex and variable mixture of asthenospheric mantle, lithospheric mantle, and crust (Table 2). YAB represent the melting of a source composed mainly of a mixture of asthenospheric mantle and HIMU-like mantle. The source of OAB-hy and OAB-ne is a mixture of asthenospheric mantle and lithospheric mantle dominated by asthenospheric mantle. Low ε_{Nd} and high $^{87}Sr/^{86}Sr$ magmas and tholeiites were derived from a lithospheric mantle source and were contaminated as they passed through the crust. This shift in isotopic values due to crustal interaction (commingling and contamination) is no more than 4 units in ε_{Nd} and 0.002 in $^{87}Sr/^{86}Sr$ and does not mask the character of the mantle source.

MANTLE AND CRUSTAL BOUNDARIES

In this section, we argue that (1) the boundary between two *crustal* provinces, the northern Colorado River extensional corridor and the amagmatic zone, corresponds in general to a *mantle* boundary between asthenospheric mantle beneath the northern Colorado River extensional corridor and lithospheric mantle beneath the amagmatic zone; (2) the mantle boundary formed between about 11 and 6 Ma, during and just after the main phase of Tertiary extension in the western Lake Mead area (9 to 12 Ma);

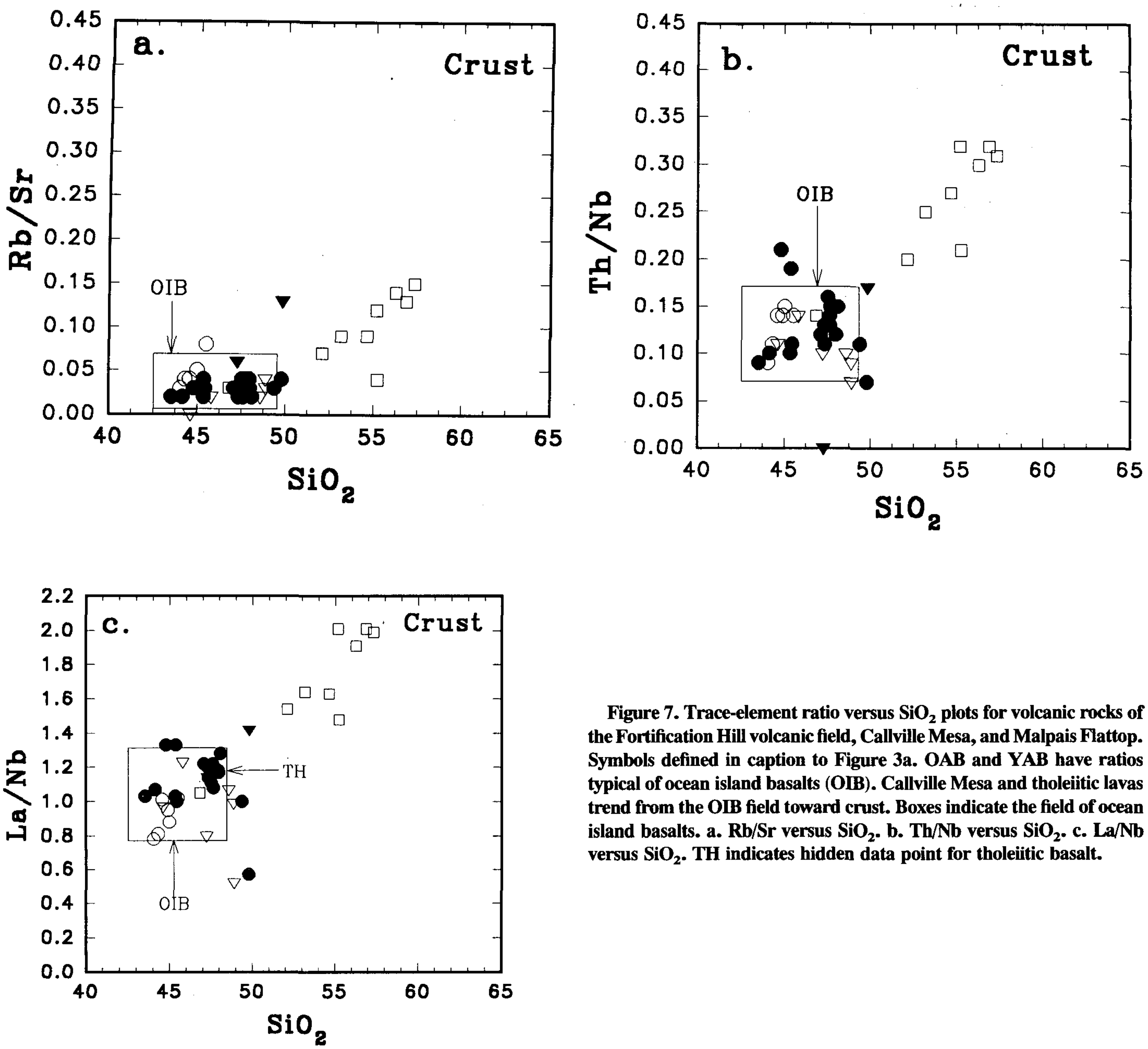

Figure 7. Trace-element ratio versus SiO_2 plots for volcanic rocks of the Fortification Hill volcanic field, Callville Mesa, and Malpais Flattop. Symbols defined in caption to Figure 3a. OAB and YAB have ratios typical of ocean island basalts (OIB). Callville Mesa and tholeiitic lavas trend from the OIB field toward crust. Boxes indicate the field of ocean island basalts. a. Rb/Sr versus SiO_2. b. Th/Nb versus SiO_2. c. La/Nb versus SiO_2. TH indicates hidden data point for tholeiitic basalt.

(3) the Lake Mead fault system may locally be the upper-crustal expression of the mantle boundary; and (4) during the peak of extension, passive rifting resulted in upwelling asthenospheric mantle beneath the northern Colorado River extensional corridor.

Our arguments below are based on the premise that depth of generation of alkali basalt magma in the study area remains relatively constant with time from 16 to 9 Ma (the period of peak extension regionally; see below). This assumption is based on the work of Takahashi and Kushiro (1983). Tholeiitic basalts are generated by partial melting of mantle peridotite with the mineral assemblage clinopyroxene, olivine, orthopyroxene at pressures of 8 to 15 kbar corresponding to depths of 24 to 45 km. Alkali basalts are produced from a similar source at pressures between 15 and 20 kbar corresponding to a depth of about 45 to 60 km. Crustal extension is accompanied by the rise of the geotherm to higher levels of the lithosphere. Therefore the expected relationship between extension and volcanism is the production of tholeiitic basalts during extension when isotherms are elevated, and alkali basalts late when isotherms relax. In the Lake Mead area, however, the most compositionally primitive basalts in any given area are generally alkalic regardless of age and relation to extension. An exception is the tholeiitic basalt at Malpais Flattop. Therefore, depth of melting appears to remain relatively constant with time, and variations in chemical and isotopic compositions are due to the rise of the lithospheric mantle–asthenosphere compositional boundary rather than significant changes in the depth of melting.

In our discussion below, we divide the mafic volcanic rocks into those that erupted during and prior to the major phase of upper-crust extension and those that erupted during

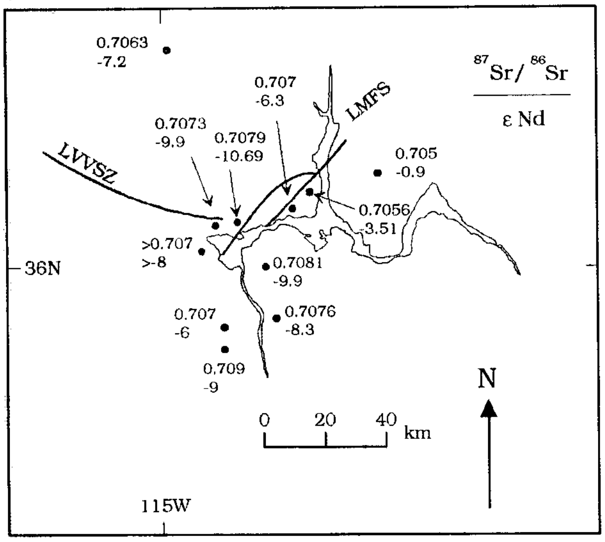

Figure 8. Map showing $^{87}Sr/^{86}Sr$ and ε_{Nd} for pre–9 Ma mafic lavas in the Lake Mead area. The amagmatic zone lies to the north of the Lake Mead fault system (LMFS); the Northern Colorado River extensional corridor is to the south. Prior to 9 Ma, isotopic values were relatively constant across the Lake Mead region and indicate that mafic volcanoes are tapping lithospheric mantle.

a period of reduced upper-crust extension. The time of peak upper-crustal extension varies across the region (Wernicke and others, 1988; Fitzgerald and others, 1992); however, in the Las Vegas–western Lake Mead area it occurred between 12 and 9 Ma (Duebendorfer and Wallin, 1991). To the south in the Eldorado and Black Mountains and to the east in the Gold Butte and Virgin Mountains, extension began at about 16 Ma (Anderson, 1971; Wernicke and others, 1988; Faulds and others, 1990). Wernicke estimated that in the Las Vegas region 75% of extension occurred between 16 and 10 Ma, and 25%, between 10 and 5 Ma. Structural information from the Lake Mead region suggests that 9 Ma is a more precise date for the termination of peak extension (Duebendorfer and Wallin, 1991). Therefore, we use 9 Ma to separate mafic lavas produced during the peak of extension from those that erupted during waning extension.

The Mantle Boundary

Isotopic data for post–9 Ma mafic lavas show regional differences that we infer to be a boundary in the magma's source region in the mantle. Contours ($^{87}Sr/^{86}Sr = 0.706$ and $\varepsilon_{Nd} = -1$) separating lavas with a dominant lithospheric mantle component ($^{87}Sr/^{86}Sr > 0.706$, $\varepsilon_{Nd} < -1$) from those with an asthenospheric mantle component ($^{87}Sr/^{86}Sr < 0.706$, $\varepsilon_{Nd} > -1$) define a boundary that extends from just north of the River Mountains into the Grand Wash trough (Fig. 8). The boundary parallels the Lake Mead fault system along most of its length and is also roughly coincident with the boundary between the northern Colorado River extensional corridor and the amagmatic zone. The regional extent of the boundary cannot be determined by isotopic techniques because of a lack of alkali basalt exposures of suitable age to the northeast and southwest of the Lake Mead area. The boundary in the Lake Mead area, however, may represent a short segment of a regionally continuous mantle boundary between asthenospheric and lithospheric mantle domains that passes through southern Nevada (Menzies, 1989). Post–9 Ma magmas tap mantle dominated by asthenospheric mantle to the south of the boundary and lithospheric mantle to the north. Because sample locations in some areas are separated by considerable distance, placement of these contours is somewhat arbitrary; however, they do define the general area of isotopic change. We suggest that this boundary formed during and just after the period of peak extension. Pre–9 Ma basalts throughout the region have uniform ε_{Nd} and $^{87}Sr/^{86}Sr$ and were derived by melting of lithospheric mantle (Fig. 9). Also, trace-element compositions of pre–9 Ma mafic lavas are similar to those basalts of the Western Great Basin province derived from lithospheric mantle (Fitton and others, 1991) (Fig. 10a). Therefore, prior to about 9 Ma, lithospheric mantle extended beneath the Lake Mead area. Post–9 Ma basalts in the northern Colorado River extensional corridor to the south of the boundary display a dramatic shift in $^{87}Sr/^{86}Sr$ and ε_{Nd}. $^{87}Sr/^{86}Sr$ changes from about 0.707 to 0.703–0.705, and ε_{Nd} changes from about -9 to higher values (-1 to $+6.7$) (Fig. 8). Chemically, mafic volcanic rocks acquire the signature of OIB lavas of the Transition Zone (Fig. 10b). In the amagmatic zone to the north of the boundary, post–9 Ma mafic lavas at Black Point and at Callville Mesa retain the isotopic signature of pre–9 Ma lavas (Fig. 8) and may represent the easternmost limit of the southern Nevada basalt field of Farmer and others (1989). Our

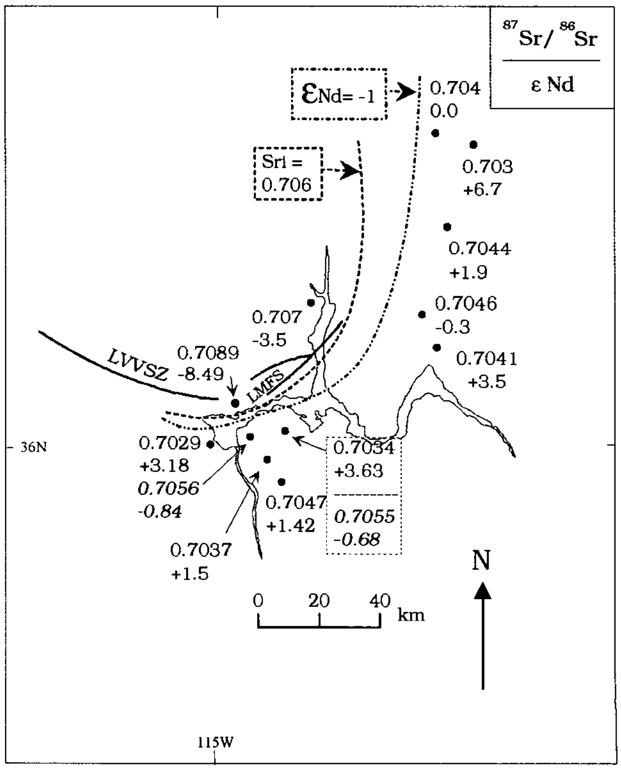

Figure 9. Map showing $^{87}Sr/^{86}Sr$ and ε_{Nd} for post–9 Ma mafic lavas in the Lake Mead area. Contours separate areas where mafic volcanoes are tapping asthenospheric mantle ($\varepsilon_{Nd} > -1$, $^{87}Sr/^{86}Sr < 0.704$) from those areas where volcanoes are tapping lithospheric mantle. Note that the Lake Mead fault system is colinear with the isotopic contours and that asthenospheric mantle is mainly present to the south in the Northern Colorado River extensional corridor. Values in italics are OAB-hy.

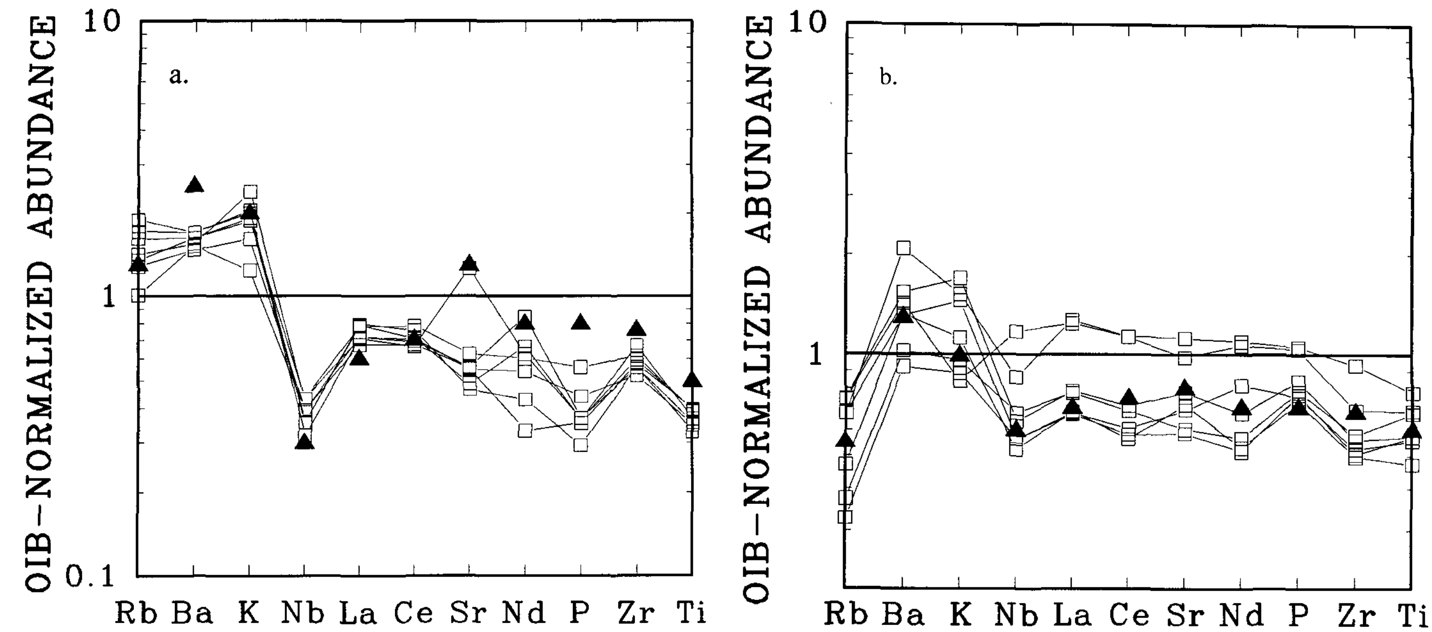

Figure 10. a. Mafic volcanic rocks in the Lake Mead area that were erupted prior to 9 Ma (open squares) are similar to lavas of the Western Great Basin province (solid triangles) produced by melting lithospheric mantle (Fitton and others, 1991). b. Spider plot of incompatible elements versus abundance normalized to OIB average of Fitton and others (1991). Post–9 Ma mafic lavas in the Northern Colorado River extensional corridor (open squares) are similar in trace-element abundance and pattern to lavas in the Colorado Plateau–Basin and Range Transition Zone derived by melting asthenospheric mantle (solid triangles) (Fitton and others, 1991).

interpretation of these data is that between 11 and about 6 Ma, the source of mafic lavas in the northern Colorado River extensional corridor changed from lithospheric mantle to asthenospheric mantle. The source of lavas in the amagmatic zone remained in the lithospheric mantle. Apparently, the lithospheric mantle was thinned or removed from beneath the northern Colorado River extensional corridor but remained intact beneath the amagmatic zone. Therefore, we infer that the mantle boundary between lithospheric mantle (north) and asthenospheric mantle (south) formed between about 11 and 6 Ma.

Mantle Plumes?

The change in source of basalts from lithospheric mantle to asthenospheric mantle with time, the OIB character of the mafic lavas, and the presence of an HIMU-type mantle component are compatible with the presence of a rising asthenospheric plume beneath the northern Colorado River extensional corridor. Mechanisms to account for lithospheric extension and OIB-type volcanism commonly call for an upwelling mantle plume (active rifting) (for example, Eaton, 1982; Fitton and others, 1991).

Unusually hot asthenosphere may not be required to induce lithospheric extension and volcanism (Buck, 1986; Perry and others, 1987; White, 1987; White and others, 1988). Mantle upwelling may be passive and caused by stretching and thinning of the lithosphere. The mantle rises to compensate for thinning crust. Melting results from the decompression of asthenospheric mantle as it rises passively beneath the stretched and thinned lithosphere. Small increases in temperature are sufficient to generate large volumes of melt during decompression. An increase of 100 °C doubles the amount of melt; 200 °C can quadruple melt volume (White and McKenzie, 1989). During passive mantle upwelling, isotopically enriched lithosphere may be thermally but not chemically converted to asthenosphere and may convectively mix with isotopically depleted asthenospheric mantle (Perry and others, 1987). OIB basalts may result from the partial melting of this two-component mantle. Hence, a deep mantle source for OIB is not required.

Passive-rifting models imply that mantle convection is coupled to the lithosphere and OIB-type volcanism may occur for long periods of time in a restricted geographic area. Perry and others (1987, 1988) applied a passive rifting model to the Rio Grande rift in central New Mexico and suggested that volcanism in the Colorado Plateau–Basin-Range transition zone may be explained by passive rifting. Recently, Bradshaw (1991) suggested a modified passive-rifting model. Plate tectonics, rather than deep-seated mantle plumes, may provide the ultimate driving force for extension and magmatism. According to Bradshaw, melting of lithospheric mantle in the northern Colorado River extensional corridor was initiated by heat input from warmer asthenosphere as it rose to fill a slab window left by the northward migration of the Mendocino triple junction.

Passive rifting is probably more applicable to the northern Colorado River extensional corridor than active rifting for two reasons. First, active plumes produce large volumes of mantle-derived melt (for example, Gallagher and Hawkesworth, 1992). Very low volumes of alkali basalt magma produced after 9 Ma in the Lake Mead area suggest that an active plume was not present during this time. Second, alkali basalt magmas in the northern Colorado River extensional corridor result from melting a three-component source composed of lithospheric mantle, asthenospheric mantle, and HIMU mantle. Lithospheric mantle was an important component in the source of older OAB-hy and low ε_{Nd} alkali basalts but becomes less important with time. This geochemical pattern is compatible with the model of passive rifting and lithospheric erosion as described by

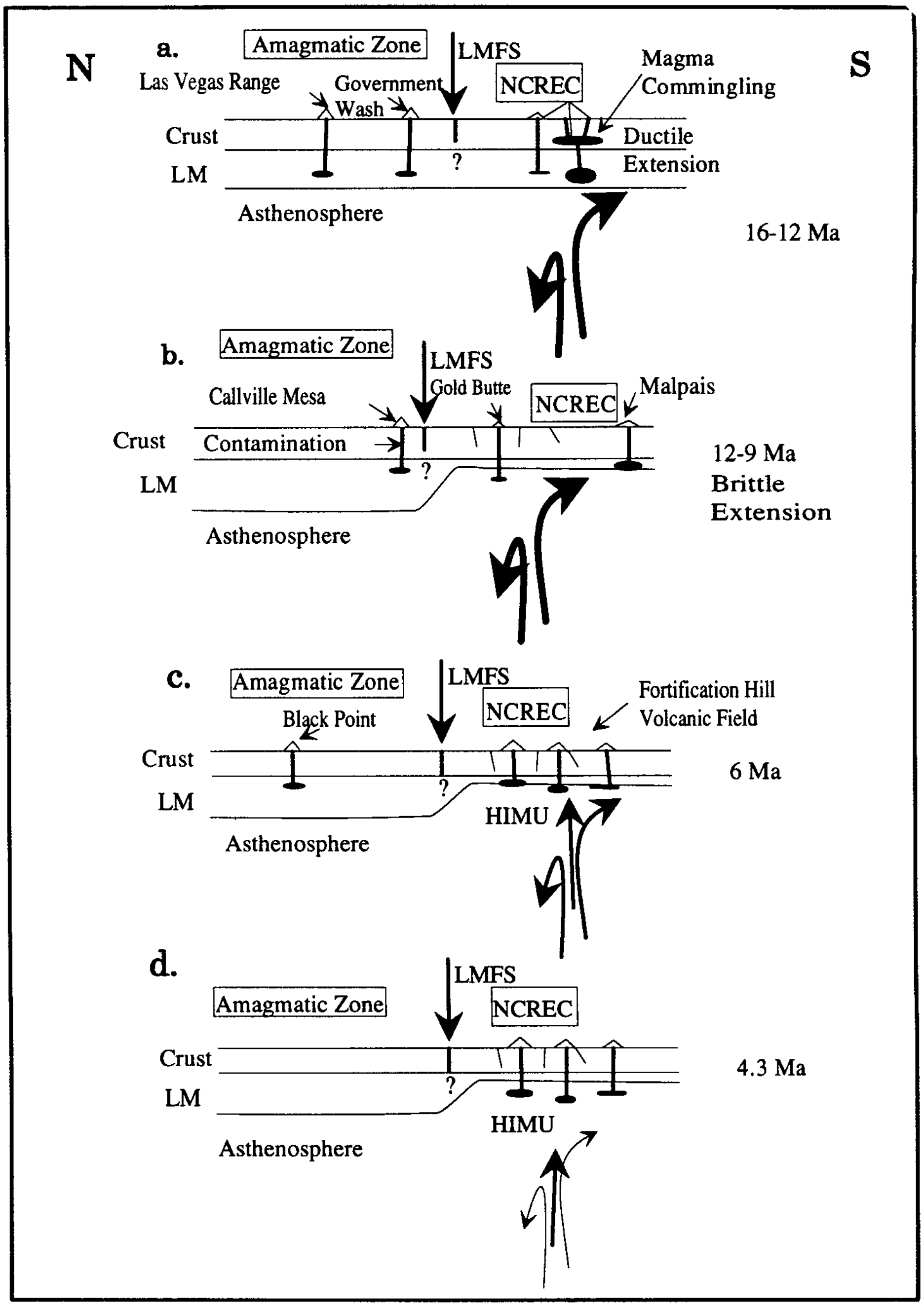

Figure 11. Summary of mantle evolution and magmatism in the Lake Mead area. Sections are diagrammatic and are roughly drawn in a north-south direction. Mantle currents and crustal extension are in an east-west direction. LMFS, Lake Mead Fault system; NCREC, northern Colorado River extensional corridor.

a. *Early Stage of Extension.* Crustal extension was initiated at about 16 Ma in the Lake Mead–Gold Butte area by either active mantle convection (Fitton and others, 1991) or the opening of a slab window (Bradshaw, 1991). Mafic magmas were generated in lithospheric mantle and locally rose to the surface without being significantly contaminated (for example, Las Vegas Range, alkali basalt in River Mountains). Mafic magma stalled in the crust at "ductile barriers" and commingled with crustal magma to form calc-intermediate volcanoes and plutons (Smith and others, 1990; Bradshaw, 1991).

b. *Peak of Extension.* Upper crustal extension occurred in the western Lake Mead portion of the northern Colorado River extensional corridor between 12 and 9 Ma but was not accompanied by significant magmatism. During extension in the northern Colorado River extensional corridor, lithospheric mantle may have been thinned and replaced by asthenosphere progressively to the west. During thinning and replacement of the lithospheric mantle in the northern Colorado River extensional corridor, the lithospheric mantle in the amagmatic zone remained intact. Contrasting behavior to the north and south of this boundary produced the mantle domain boundary. The Lake Mead fault system is spatially and temporally related to the mantle boundary. The Lake Mead fault system may be the crustal manifestation of differential thinning of the lithospheric mantle. Mantle convection between 12 and 9 Ma is probably passive and is driven by crustal thinning.

c. *After the Peak of Extension.* After the peak of extension, volcanism in the northern Colorado River extensional corridor originates in the asthenosphere near the boundary with the lithospheric mantle at a depth of 45 to 60 km. In the amagmatic zone, mafic volcanic rocks at Black Point originate in the lithospheric mantle. Isotopic compositions of alkali basalts define two mantle domains. The domain to the north is characterized by lithospheric mantle (ε_{Nd} = −3 to −9; $^{87}Sr/^{86}Sr$ = 0.706–0.707). To the south, mafic lavas have an OIB-mantle signature and appear to have only a minor lithospheric mantle component in their source (ε_{Nd} = 0 to +4; $^{87}Sr/^{86}Sr$ = 0.703–0.705). The change in source of basalts from lithospheric mantle to asthenospheric mantle with time, the OIB character of the mafic lavas, and the presence of an HIMU-like mantle component is compatible with the presence of rising asthenosphere, as an upwelling convective cell, or plume beneath the northern Colorado River extensional corridor at 6 Ma after the peak of extension.

d. *After Extension.* Low-volume xenolith-bearing alkali basalts formed in the northern Colorado River extensional corridor by melting asthenosphere mixed with an HIMU-like component. Because lithospheric thinning is unlikely at 4.3 Ma, the lower proportion of lithospheric mantle in the source of alkali basalts and the higher proportion of HIMU-like mantle suggest that the depth of melting increased between 6 and 4.3 Ma. Passive rifting may have continued as late as 4.3 Ma as evidenced by the presence of the HIMU-like mantle component in mafic lavas of this age.

Perry and others (1987) for the Rio Grande Rift.

Passive rifting may have been preceded by active rifting in the northern Colorado River extensional corridor. Faulds and others (1990) suggested that upwelling was active in the northern Colorado River extensional corridor during mid-Miocene extension. Faulds and others (1990) developed a kinematic model that implies that extension (spreading) occurred about discrete axes and that highly extended areas lie directly above areas of divergent flow in the asthenosphere. Alternatively, passive rifting between 11 and 6 Ma may have been a continuation of an earlier more intense passive rifting event related to the opening of a slab window left by the northward migration of the Mendocino triple junction (Bradshaw, 1991).

Links between Mantle and Crust

$^{87}Sr/^{86}Sr = 0.706$ and $\varepsilon_{Nd} = -1$ contours trend east-northeast and are roughly coincident with the Lake Mead fault system (Fig. 8). The correspondence between isotopic contours and the Lake Mead fault system is especially good just north of Lake Mead where there are numerous isotopic data points and tighter control of the location of the contours (Fig. 8). The Lake Mead fault system is a set of northeast-striking left-lateral faults with 65 km of cumulative slip that occurred between 17 and 10 Ma (Anderson, 1973; Bohannon, 1979, 1984). Weber and Smith (1987) considered the Lake Mead fault system and the Saddle Island detachment (Smith, 1982; Duebendorfer and others, 1990) to be a kinematically coordinated system of faults. If the Weber and Smith (1987) model is correct, then the Lake Mead fault system is a shallow crustal structure. Recently, Smith and others (1991) suggested that the Saddle Island fault originated as a steeply dipping normal fault and that the Lake Mead fault system represents the northern boundary of the Saddle Island allochthon. In this case, the Lake Mead fault system may extend into the middle to lower crust. Faulds and others (1990) considered both the Lake Mead fault system and the Las Vegas Valley shear zone as the northern boundary of the northern Colorado River extensional corridor and as corresponding to intracontinental transform faults separating *en echelon* axes of extension. We suggest that the similar trend and geographic location of the isotopic boundaries and the Lake Mead fault system argue for a genetic relationship between the two features. The Lake Mead fault system may represent the crustal manifestation of differential thinning of the lithospheric mantle or the rejuvenation of an older lithospheric structure. Whatever the connection, it appears that the Lake Mead fault system reflects mantle processes and may be an important deeply penetrating (?) crustal structure.

SUMMARY

The formation of a mantle domain boundary is depicted on four diagrammatic north-south sections across the Lake Mead area (Fig. 11). The sections display the interaction of mantle and crust during the early stage of extension in the Lake Mead area (16–12 Ma), during the peak of extension (12–9 Ma), after the peak of extension during the eruption of Fortification Hill basalts (6 Ma), and after extension during the eruption of xenolith-bearing alkali basalts (4.3 Ma).

ACKNOWLEDGMENTS

This research was supported by a grant from the Nevada Nuclear Waste Project Office. We thank James Faulds and Terry Naumann for informative discussions and for reading early versions of this paper. Ernie Duebendorfer, Scott Vetter, and John Shervais provided reviews that helped improve the quality and clarity of the paper. We thank the staff of the Phoenix Memorial Laboratory, University of Michigan, for completing the REE analyses and Dave Nealey (U.S. Geological Survey) for arranging for XRF analyses of selected samples. Partial laboratory support at the University of Kansas was provided by National Science Foundation Grant EAR-8904007 awarded to Walker. We thank Randy Van Schmus and Drew Coleman for helpful discussions concerning the collection of the isotopic data.

REFERENCES CITED

Anderson, R. E., 1971, Thin skin distension in Tertiary rocks of southeastern Nevada: Geological Society of America Bulletin, v. 82, p. 42–58.

Anderson, R. E., 1973, Large-magnitude late Tertiary strike-slip faulting north of Lake Mead, Nevada: U.S. Geological Survey Professional Paper 794, 18 p.

Anderson, R. E., Longwell, C. R., Armstrong, R. L., and Marvin, R. F., 1972, Significance of K-Ar ages of Tertiary rocks from the Lake Mead region, Nevada-Arizona: Geological Society of America Bulletin, v. 83, p. 273–288.

Armstrong, R. L., 1966, K-Ar dating using neutron activation for Ar analysis: Geochimica et Cosmochimica Acta, v. 30, p. 565–600.

Armstrong, R. L., 1970, Geochronology of Tertiary igneous rocks, eastern Basin and Range province, western Utah, eastern Nevada, and vicinity, U.S.A.: Geochimica et Cosmochimica Acta, v. 34, p. 203–232.

Barker, D. S., and Thompson, K. G., 1989, Hamblin-Cleopatra volcano, Nevada: Genesis of a shoshonite-latite-trachydacite-trachyte suite, *in* Continental magmatism abstracts, IAVCEI: New Mexico Institute of Mining and Geology Bulletin 131, p. 17.

Bennett, V. C., and DePaolo, D. J., 1987, Proterozoic crustal history of the western United States as determined by Nd isotopic mapping: Geological Society of America Bulletin, v. 99, p. 674–685.

Bohannon, R. G., 1979, Strike-slip faults of the Lake Mead region of southern Nevada, *in* Armentrout, J. M., Cole, M. R., and Terbest, H., eds., Cenozoic paleogeography of the western United States: Pacific Section, Society of Economic Paleontologists and Mineralogists Pacific Coast Paleogeography Symposium 3, p. 129–139.

Bohannon, R. G., 1984, Nonmarine sedimentary rocks of Tertiary age in the Lake Mead region: U.S. Geological Survey Professional Paper 1259, 72 p.

Bradshaw, T. K., 1991, Tectonics and magmatism in the Basin and Range province of the western United States [Ph.D. dissert.]: Milton Keynes, Great Britain, The Open University, 247 p.

Buck, W. R., 1986, Small-scale convection induced by passive rifting: The cause for uplift of rift shoulders: Earth and Planetary Science Letters, v. 77, p. 362–372.

Campbell, I., and Schenk, E. T., 1950, Camptonite dikes near Boulder Dam, Arizona: American Mineralogist, v. 35, p. 671–692.

Cascadden, T. E., 1991, Style of volcanism and extensional tectonics in the eastern Basin and Range province: Northern Mohave County, Arizona [M.S. thesis]: Las Vegas, Nevada, University of Nevada, 156 p.

Cascadden, T. E., and Smith, E. I., 1991, Intermediate and mafic volcanic rocks of the northern White Hills, Arizona: Implications for the production of intermediate composition volcanic rocks during regional extension: Geological Society of America Abstracts with Programs, v. 23, no. 5, p. 390.

Cole, E. D., 1989, Petrogenesis of late Cenozoic alkalic basalt near the eastern boundary of the Basin-and-Range: Upper Grand Wash trough, Arizona and Gold Butte, Nevada [M.S. thesis]: Las Vegas, Nevada, University of Nevada, 68 p.

Cooper, J. L., and Hart, W. K., 1990, Mantle sources in the Arizona transition zone and global mantle heterogeneity: Geology, v. 18, p. 1146–1149.

Crowley, J. C., 1984, Strontium isotope and rare earth element analysis of Rio Grande rift basalts: Implications for magmagenesis in continental rifts [Ph.D. dissert.]: Providence, Rhode Island, Brown University, 116 p.

Daley, E. E., and DePaolo, D. J., 1992, Isotopic evidence for lithospheric thinning during extension: Southeastern Great Basin: Geology, v. 20, p. 104–108.

Darvall, P., Gans, P. B., and Lister, G. S., 1991, Normal faulting in the Eldorado Mountains, southeastern Nevada: Geological Society of America Abstracts with Programs, v. 23, no. 2, p. 17.

Duebendorfer, E. M., and Wallin, E. T., 1991, Basin development and syntectonic sedimentation associated with kinematically coupled strike-slip and detachment faulting, southeastern Nevada: Geology, v. 19, p. 87–90.

Duebendorfer, E. M., Shafiqullah, M., and Damon, P. E., 1991a, The Las Vegas Valley Shear Zone: A middle to late Miocene extensional transfer fault: Geological Society of America Abstracts with Programs, v. 23, no. 5, p. A188.

Duebendorfer, E. M., Sewall, A. J., and Smith, E. I., 1991b, The Saddle Island Detachment fault, an evolving shear zone in the Lake Mead area of southern Nevada, *in* Wernicke, B., ed., Mid-Tertiary extension at the latitude of Las Vegas: Geological Society of America Memoir 176, p. 77–97.

Dungan, M. A., 1992, Interpretation of elemental and isotopic signatures of extension-related basalts: Implications of Northern Rio Grande Rift volcanism [abs.]: American Geophysical Union Transactions, v. 73, no. 10, p. 334.

Eaton, G. P., 1982, The Basin and Range province: Origin and tectonic significance: Annual Review of Earth and Planetary Sciences, v. 10, p. 409–440.

Eaton, G. P., Wahl, R. R., Prostka, H. J., Mabey, D. R., and Kleinkopf, M. D., 1978, Regional gravity and tectonic patterns: Their relation to late Cenozoic epeirogeny and lateral spreading in the western Cordillera, *in* Smith, R. B., and Eaton, G. P., eds., Cenozoic tectonics and regional geophysics of the Western Cordillera: Geological Society of America Memoir 152, p. 51–93.

Farmer, G. L., Perry, F. V., Semken, S., Crowe, B., Curtis, D., and DePaolo, D. J., 1989, Isotopic evidence of the structure and origin of subcontinental lithospheric mantle in southern Nevada: Journal of Geophysical Research, v. 94, p. 7885–7898.

Faulds, J. E., Geissman, J. W., and Mawer, C. K., 1990, Structural development of a major extensional accommodation zone in the Basin and Range province, northwestern Arizona and southern Nevada; Implications for kinematic models of continental extension, *in* Wernicke, B. P., ed., Basin and Range extensional tectonics near the latitude of Las Vegas, Nevada: Geological Society of America Memoir 176, p. 37–76.

Faulds, J. E., Feuerbach, D. L., and Smith, E. I., 1991, New insights on structural controls and emplacement mechanisms of Pliocene/Quaternary basaltic dikes, southern Nevada and northwestern Arizona: Geological Society of America Abstracts with Programs, v. 23, no. 5, p. 118.

Feuerbach, D. L., Smith, E. I., Shafiqullah, M., and Damon, P. E., 1991, New K-Ar dates for late-Miocene to early Pliocene mafic volcanic rocks in the Lake Mead area, Nevada and Arizona: Isochron West, no. 57, p. 17–20.

Fitton, J. G., James, D., Kempton, P. D., Ormerod, D. S., and Leeman, W. P., 1988, The role of lithospheric mantle in the generation of late Cenozoic basic magmas in the western United States: Journal of Petrology, Special Lithosphere Issue, p. 331–349.

Fitton, J. G., James, D., and Leeman, W. P., 1991, Basic magmatism associated with Late Cenozoic extension in the western United States: Compositional variations in space and time: Journal of Geophysical Research, v. 96, no. B8, p. 13,693–13,711.

Fitzgerald, P. G., Fryxell, J. E., and Wernicke, B. P., 1991, Miocene crustal extension and uplift in southeastern Nevada: Constraints from fission track analysis: Geology, v. 19, p. 1013–1016.

Glazner, A. F., and Farmer, G. L., 1991, Production of isotopic variability in basalts by cryptic mafic contamination: Transactions of the American Geophysical Union, v. 72, p. 267.

Glazner, A. F., and Farmer, G. L., 1992, Production of isotopic variability in continental basalts as cryptic crustal contamination: Science, v. 255, p. 72–74.

Glazner, A. F., and Supplee, J. A., 1982, Migration of Tertiary volcanism in the southwestern United States and subduction of the Mendocino fracture zone: Earth and Planetary Science Letters, v. 60, p. 429–436.

Hart, S. R., 1988, Heterogeneous mantle domains: Signatures, genesis and mixing chronologies: Earth and Planetary Science Letters, v. 90, p. 273–296.

Hart, S. R., Hauri, E. H., Oschmann, L. A., and Whitehead, J. A., 1992, Mantle plumes and entrainment: Isotopic evidence: Science, v. 256, p. 517–520.

Hart, W. K., 1985, Chemical and isotopic evidence for mixing between depleted and enriched mantle, northwestern U.S.A.: Geochimica et Cosmochimica Acta, v. 49, p. 131–144.

Leat, P. T., Thompson, R. N., Dicken, A. P., Morrison, M. A., and Hendry, G. L., 1989, Quaternary volcanism in northwestern Colorado: Implications for the roles of asthenosphere and lithosphere in the genesis of continental basalts: Journal of Volcanology and Geothermal Research, v. 37, p. 291–310.

Leat, P. T., Thompson, R. N., Morrison, M. A., Hendry, G. L., and Dicken, A. P., 1991, Alkaline hybrid mafic magmas of the Yampa area, NW Colorado, and their relationship to the Yellowstone mantle plume and lithospheric mantle domains: Contributions to Mineralogy and Petrology, v. 107, p. 310–327.

Leeman, W. P., 1970, Late Cenozoic alkali-olivine basalts of the Basin-Range province, USA: Contributions to Mineralogy and Petrology, v. 25, p. 1–24.

Longwell, C. R., 1960, Possible explanation of diverse structural patterns in southern Nevada: American Journal of Science, v. 258-A (Bradley Volume), p. 192–203.

Longwell, C. R., Pampeyan, E. H., Bower, B., and Roberts, R. J., 1965, Geology and mineral deposits of Clark County, Nevada: Nevada Bureau of Mines and Geology Bulletin 62, 218 p.

Menzies, M. A., 1989, Cratonic, circumcratonic and oceanic mantle domains beneath the western United States: Journal of Geophysical Research, v. 94, p. 7899–7915.

Menzies, M. A., Leeman, W. P., and Hawkesworth, C. J., 1983, Isotope geochemistry of Cenozoic volcanic rocks reveals mantle heterogeneity below western U.S.A.: Nature, v. 303, p. 205–209.

Mills, J. G., 1985, The geology and geochemistry of volcanic and plutonic rocks in the Hoover Dam 7.5 minute quadrangle, Clark County, Nevada and Mojave County, Arizona [M.S. thesis]: Las Vegas, Nevada, University of Nevada, 119 p.

Naumann, T. R., 1987, Geology of the central Boulder Canyon quadrangle, Clark County, Nevada [M.S. thesis]: Las Vegas, Nevada, University of Nevada, 68 p.

Naumann, T. R., and Smith, E. I., 1987, Evidence for magma mixing in mid-Tertiary rocks, Lake Mead region, southern Nevada: Geological Society of America Abstracts with Programs, v. 19, p. 435–436.

Perry, F. V., Baldridge, W. S., and DePaolo, D. J., 1987, Role of asthenosphere and lithosphere in the genesis of late Cenozoic basaltic rocks from the Rio Grande Rift and adjacent areas of the southwestern United States: Journal of Geophysical Research, v. 92, p. 9193–9213.

Reynolds, S. J., Florence, F. P., Welty, J. W., Roddy, M. S., Currier, D. A., Anderson, B. V., and Keith, S. B., 1986, Compilation of radiometric age determinations in Arizona: Arizona Bureau of Geology and Mineral Technology Bulletin 197, 258 p.

Smith, E. I., 1982, Geology and geochemistry of the volcanic rocks in the River Mountains, Clark County, Nevada and comparisons with volcanic rocks in nearby areas, *in* Frost, E. G., and Martin, D. L., eds., Mesozoic-Cenozoic tectonic evolution of the Colorado River region, California, Arizona, and Nevada: San Diego, California, Cordilleran Publishers, p. 41–54.

Smith, E. I., 1984, Geological map of the Boulder Beach Quadrangle, Nevada: Nevada Bureau of Mines and Geology Map 81, scale 1:24,000.

Smith, E. I., Schmidt, C. S., and Mills, J. G., 1988, Mid-Tertiary volcanoes of the Lake Mead area of southern Nevada and northwestern Arizona, *in* Weide, D. L., and Faber, M. L., eds., This extended land, Geological journeys in the southern Basin and Range: Geological Society of America, Cordilleran Section field trip guidebook: University of Nevada, Las Vegas, Department of Geoscience Special Publication No. 2, p. 107–122.

Smith, E. I., Feuerbach, D. L., Naumann, T. R., and Mills, J. G., 1990, Geochemistry and evolution of mid-Miocene igneous rocks in the Lake Mead area of Nevada and Arizona, *in* Anderson, J. L., ed., Cordilleran magmatism: Geological Society of America Memoir 176, p. 169–194.

Smith, E. I., Feuerbach, D. L., and Duebendorfer, E. M., 1991, Magmatism, extensional tectonics and sedimentation in the Lake Mead area of Nevada and Arizona: A new model: Geological Society of America Abstracts with Programs, v. 23, p. 63.

Takahashi, E., and Kushiro, I., 1983, Melting of dry peridotite at high pressures and basalt magma genesis: American Mineralogist, v. 68, p. 859–879.

Taylor, W. J., and Bartley, J. M., 1988, Prevolcanic extensional breakaway zone, east-central Nevada: Geological Society of America Abstracts with Programs, v. 19, p. 457.

Thompson, K. G., 1985, Stratigraphy and petrology of the Hamblin-Cleopatra volcano, Clark County, Nevada [M.S. thesis]: Austin, Texas, University of Texas, 306 p.

Walker, J. D., and Coleman, D. S., 1991, Geochemical constraints on mode of extension in the Death Valley region: Geology, v. 19, no. 10, p. 971–974.

Weaver, B. L., 1991a, The origin of ocean island basalt end-member compositions: Trace element and isotopic constraints: Earth and Planetary Science Letters, v. 104, p. 381–397.

Weaver, B. L., 1991b, Trace element evidence for the origin of ocean-island basalts: Geology, v. 19, p. 123–126.

Weaver, B. L., Wood, D. A., Tarney, J., and Joron, J. L., 1986, Role of subducted sediment in the genesis of ocean island basalts: Geochemical evidence from South Atlantic Ocean Islands: Geology, v. 14, p. 275–278.

Weber, M. E., and Smith, E. I., 1987, Structural and geochemical constraints on the reassembly of disrupted mid-Miocene volcanoes in the Lake Mead–Eldorado Valley area of southern Nevada: Geology, v. 15, p. 553–556.

Wernicke, B., and Axen, G. J., 1988, On the role of isostasy in the evolution of normal fault systems: Geology, v. 16, p. 848–861.

White, R. S., 1987, The earth's crust and lithosphere: Journal of Petrology, Special Lithosphere Issue, p. 1–10.

White, R. S., and McKenzie, D. P., 1989, Magmatism at rift zones: The generation of volcanic continental margins and flood basalts: Journal of Geophysical Research, v. 94, p. 7685–7730.

White, R. S., Spence, G. D., Fowler, S. R., McKenzie, D. P., Westbrook, G. K., and Bowen, A. D., 1988, Magmatism at rifted continental margins: Nature, v. 330, p. 439–444.

White, W. M., and Patchet, P. J., 1984, Hf-Nd-Sr isotopes and incompatible element abundances in island arcs: Implications for magma origins and crust-mantle evolution: Earth and Planetary Science Letters, v. 67, p. 167–185.

Wooden, J. L., and Miller, D. M., 1990, Chronologic and isotopic framework for early Proterozoic crustal evolution in the eastern Mohave Desert region, SE California: Journal of Geophysical Research, v. 95, no. B12, p. 20,133–20,146.

Zindler, A., and Hart, S. R., 1986, Chemical geodynamics: Annual Review of Earth and Planetary Science Letters, v. 14, p. 493–571.

Manuscript Received by the Society August 24, 1992
Revised Manuscript Received April 5, 1993
Manuscript Accepted April 15, 1993

Printed in U.S.A.